TEXAS A&M UNIVERSITY
LOW SPEED WIND TUNNEL

FURTHER WIND TUNNEL INVESTIGATION OF THE SM701 AIRFOIL WITH AILERON AND TURBULATORS

By:
Gregory Steen
Oran Nicks
Michael Heffner

College Station, Texas

August 1992

Texas A&M University

Low Speed Wind Tunnel

FURTHER WIND TUNNEL INVESTIGATION OF THE SM701 AIRFOIL WITH AILERON AND TURBULATORS

By:

Gregory Steen, Research Specialist and Graduate Student

Oran Nicks, Research Engineer

Michael Heffner, Undergraduate Student

ABSTRACT

Wind tunnel tests were performed on a two-dimensional model of the SM701 airfoil designed for use on the World Class gliders. The test covered a range of Reynolds Numbers from 500,000 to 1.7 million. Aerodynamic forces and moments were measured with an external balance. Momentum loss method measurements of the section drag coefficient were also made. Flow visualization techniques provided information on transition from laminar to turbulent flow. Lift, drag, and pitching moment were analyzed and comparisons were made with predicted and previously obtained experimental data. The effects of V-tape turbulators for use in turbulent drag reduction were studied. The performance of a 25% chord aileron deflected through ±20° was researched. The model was designed, constructed, and the test conducted by students at Texas A&M University.

SYMBOLS

AR	aspect ratio
a/c	alternating current
bal	external balance
C_D	drag coefficient
C_L	lift coefficient
C_{Lmax}	maximum lift coefficient
C_m	pitching moment coefficient
d/c	direct current
ft	feet
Hz	Hertz
in	inch
KVA	kilovolt-amps
lbs	pounds
mom	momentum loss method
psf	pounds per square foot
q	dynamic pressure
q_{act}	actual dynamic pressure
q_{set}	set dynamic pressure
RN	Reynolds Number
RPM	revolutions per minute
W	uncertainty
α	angle of attack
α_0	zero lift angle of attack
δ_A	aileron deflection angle

INTRODUCTION

The International Gliding Commission (IGC) of the Federation Aeronautique Internationale (FAI) initiated a design and prototype competition in 1989 for a new World Class glider to be used in international competition. Technical Specifications for this design and ground rules for the competition were announced worldwide by the FAI. The specifications were prepared by an international

panel incorporating judgments that favor low cost, safety, suitable performance, and ease of handling that might encourage soaring on a worldwide basis.[1]

The balanced characteristics chosen by the panel suggested the desirability of a high maximum lift coefficient, gentle stall and adequate L/D ratios at low Reynolds Numbers. Mr. Dan M. Somers and Dr. Mark D. Maughmer teamed to design a suitable airfoil, taking into account the compromises involved in World Class Technical Specifications. The SM701 airfoil was designed using The Eppler Airfoil Program System. Its physical and design characteristics were then offered to all designers who might wish to employ this new section.[2]

The two-dimensional performance characteristics of the airfoil were experimentally and numerically verified by a student research team at Texas A&M University through NASA Grant NAG-1260-FDP.[3,4] During the test, some ideas for improvements were developed. The students constructed the previous model by modifying an existing two-dimensional airfoil model donated to the University. This was accomplished by gloving over the previous shape with foam, sanding to the new profile, covering the surface with fiberglass, and using body filler to achieve the final shape. Because the model was a modification of a previous wing section, it was necessary to extend the chord to approximately 32 inches. A primary shortcoming of the original test was the inability of the tunnel to provide good flow quality and stable dynamic pressures at the extremely low velocities required to test at the lowest Reynolds Number cases. Therefore, a new model with a smaller chord more suited to the low Reynolds Number studies was built. Since some form of turbulent drag reduction is common on many sailplanes, the students felt a study attempting to lower the drag values of this airfoil through the use of additional drag reduction methods would be beneficial. It was also determined that aileron deflection information would be valuable for a sailplane designer wishing to employ this section.

Incorporating the previous experiences with ideas for improvements and further study, the students and advisors proposed an additional wind tunnel test of the SM701. This test used a new model of the SM701 specifically designed for this project. The two-dimensional model has a 16 inch chord, thus allowing studies in the 500,000 to 1.7 million Reynolds Number range. Provisions for a 25% chord moveable aileron were also included in the new design.

FACILITY DESCRIPTION

The Texas A&M University Low Speed Wind Tunnel (TAMU-LSWT) is a self contained research facility located adjacent to Easterwood Airport in College Station, Texas.[5] It is owned and operated by the Aerospace Engineering Division of the Texas Engineering Experiment Station.

The wind tunnel is of the closed circuit, single return type having a rectangular test section ten feet wide and seven feet high. Figure 1 presents a line drawing of the second floor of the building and a plan view of the wind tunnel circuit. Total circuit length at the centerline is 396 feet. The maximum diameter of 30 feet occurs in the settling chamber. A single screen located at the settling chamber entrance and a double screen just upstream of the contraction section are used to improve dynamic pressure uniformity and to reduce flow turbulence levels.

The contraction section which acts as a transition piece from circular to rectangular cross section is of reinforced concrete construction. The contraction ratio is 10.4 to 1 in a length of 30 feet.

Diffusion takes place immediately downstream of the test section in a concrete diffuser which also returns the flow to a circular cross-section. The horizontal expansion angle is 1.43 degrees and the vertical 3.38 degrees in an overall length of 46.5 feet.

A 12.5 foot diameter, four-blade Curtiss Electric propeller driven at 900 RPM by a 1250 KVA synchronous electric motor provides the air flow in the wind tunnel. Any desired test section dynamic pressure between zero and 100 pounds per square foot can be obtained by proper blade pitch angle positioning.

Separate studies were conducted on the freestream turbulence intensity levels in the test section.[6] Consultation with NASA Langley engineers provided insight and guidance into the most appropriate method of acquiring and reducing this data. The data was acquired using a TSI single component hot film probe and associated anemometer circuitry. The signal from the anemometer was split into a/c and d/c

components. The a/c component was then amplified approximately 120 times and these signals were read by the tunnel's Preston analog to digital converter system. The A/D system acquired 8192 samples of each channel at 4000 Hz. The a/c signal was filtered below 1 Hz and above 2000 Hz. The final results can be seen in Figure 2. The SM701 airfoil was tested in the low turbulence intensity range of 4 psf to 45 psf dynamic pressure. The turbulence intensity is fairly constant at about 0.2% through this range.

MODEL DESCRIPTION

The SM701 airfoil is a 16 percent thick, laminar flow airfoil designed for high maximum lift and low profile drag while exhibiting docile stall characteristics. The model constructed for this test had a span of 83.75 in. (6.979 ft), a chord of 16 in. (1.333 ft) and an area of 9.303 ft^2. A full span aileron was also included in the aft 25% of the chord.

The model was constructed out of foam and fiberglass built around a steel backbone. The support structure for the main wing body consisted of a 2 x 4 x 0.25 in. steel tubing spar, four 0.25 in. thick steel templates and two 0.5 in. steel templates. The aileron was also supported by four 0.25 in. steel templates and two 0.5 in. steel templates. The aileron templates were connected to the templates of the main wing by a 0.5 in. diameter steel rod. The rod was used as the hinge pin about which the aileron was deflected and it was located at 75% chord. Located approximately 1 in. behind the hinge pin was a 0.25 in. diameter steel rod used to provide extra support to the foam which was used to shape the aileron (Figures 3a-b).

The airfoil shape was generated on a computer and glued to the 0.25 in. and 0.5 in. steel plates. Approximately 0.04 in. was removed from the thickness on both the upper and lower surfaces to account for the thickness of the fiberglass. An extra 0.04 in. was removed from the lower surface just aft of the leading edge to allow for the fiberglass from the upper surface to wrap around the leading edge and overlap with the fiberglass of the lower surface. The steel plates were cut with a band saw around the airfoil shape and sanded smooth to the final shape. Templates for the aileron and the main wing body were cut separately. Once the templates were made, they were welded to the main spar at even intervals approximately 1.167 ft apart. The 0.5 in. templates were used at the ends of the wing span and the 0.25 in. templates were spaced evenly in between. A reference point on the templates was chosen and used to make sure each template was welded to the spar in line with one another. After the main wing templates were welded to the spar, the aileron templates were connected to the main wing templates with the pivot hinge. The trailing edges of the aileron templates were lined up with one another and welded to the 0.25 in. supporting rod (Figure 4).

Once the support structure was welded together, foam was laid in sections between the templates on both the upper and lower surfaces. The main wing and the aileron were shaped separately by gluing foam to the surrounding templates and the main spar or the 0.25 in. diameter support rod respectively. The foam was sanded to shape one section at a time. Since the hinge pin required easy removal and insertion, it was covered with mold release wax and expandable foam was poured in between the templates to form the leading edge of the aileron. Once the foam had set around the hinge pin, it was removed and cleaned and the leading edge was sanded to shape.

The leading edge of the aileron was covered with fiberglass first. This was done because as the aileron was deflected, various parts of its leading edge were exposed to the flow. This fiberglass was trimmed, shaped and sanded smooth. The aileron was then attached to the main wing body with the hinge pin. Brackets were mounted to the outside of the 0.5 in. templates at the ends of the wing with one bracket mounted to the aileron template and another mounted to the main wing body template. Between these brackets, connecting bars were made of varying lengths to set and fix the aileron at certain deflection angles (Figure 5).

Once the brackets were finished, the aileron was set at zero deflection. The upper and lower surfaces were covered with three layers of fiberglass and sanded smooth. Templates were made of the outer shapes of the upper and lower surfaces and placed over each to check the model shape against the expected contour. Bondo body filler was used to fill in the shape where needed. Once the final shape was obtained, it was finish sanded, painted and wet sanded smooth with 600 grit sandpaper.

A steel mounting plate was welded to the main spar and bolted to the external balance. The mounting strut was set at a level which allowed a 0.125 in. gap between the model and both the ceiling and the floor. A floor plate was cut to fit around the 2 x 4 in. steel spar and under the wing eliminating any air from flowing between the test section and the balance room (Figure 6).

The actual coordinates of the model as tested were obtained using a dial indicator. The model was clamped to the table of a milling machine and the dial indicator was clamped at a fixed height above the surface of the model. The tip of the dial indicator was moved to the airfoil leading edge and set to zero. The model was then moved chordwise under the dial indicator by moving the table of the milling machine. The x-coordinate of the dial indicator was measured using the scale on the milling machine table which could be read to 0.001 inch. The y-coordinate was read directly from the dial indicator which could also be read to 0.001 inch. This procedure was done at numerous stations along the chord of the airfoil for both the upper and lower surfaces. The coordinates obtained from these measurements were then entered into the computer and plotted out with the theoretical coordinates. Comparisons were made between these two shapes to determine the differences (Figure 7). The nose of the model was more blunt than the theoretical shape by approximately 0.16%. Along the upper surface, the model was under contour between 0.071c and 0.675c with a maximum deviation in this range of 0.13%. Between 0.675c and 0.83c, the upper surfaces matched well. From 0.83c to the trailing edge, the model was again under contour by approximately 0.16%. Along the lower surface, the model was over contour between 0.011c and 0.115c by about 0.08%. From 0.364c to 0.837c, the model was under contour by 0.24%. The remaining part of lower surface matched well.

Eppler code results obtained for the actual model coordinates are compared to the design SM701 results at RN = 1 million in Figures 8a-c. The computed C_{Lmax} is 1.756 for the designed shape and 1.711 for the actual shape. The design shape had a wider drag bucket than the model by 1° on either side, but the results were generally very close. The minimum C_D for the actual shape was 0.0065 at α = -3° and the minimum C_D for the design shape was 0.0064 at α = -5°. The pitching moment coefficients agreed well with the model results slightly less negative than the design results. It should be noted that the design shape has no trailing edge thickness while the actual shape has a finite thickness of 0.02 inches.

INSTRUMENTATION

Wake rake pressures were acquired to obtain airfoil drag coefficient data. The pressures were measured by a Pressure Systems, Inc. PSI-8400 system. The expected system accuracy is ±0.2 psf. Total and static pressure probes were located one chord length aft of the airfoil trailing edge. The probes were remotely moved through a sweep to obtain the wake profiles by the facility's traversing mechanism.

Force and moment measurements were also made with the TAMU-LSWT external balance. This six component pyramidal type balance measures each force and moment independently. Separate studies have verified the system accuracy to ±0.05 lbs. for drag force. The accuracy has been shown to be ±0.1 lbs. or ft-lbs. for readings less than 100 lbs. and ±0.1% of the reading for measurements greater than 100 lbs for all other forces and moments.

Uncertainties in each of the data types have been estimated based on the method of Reference 7. The calculated results at α = 0° are presented in Table 1. A sample of the momentum loss drag coefficient data with corresponding error bars is presented in Figure 9.

A Perkin-Elmer 3210 super-mini computer was used to acquire, process, and store all digital data.

TEST CONDITIONS

Angle of attack sweeps were run on the SM701 airfoil at five different dynamic pressures. Six component external balance data was taken at angles of attack from negative stall through positive stall in one degree increments. The set dynamic pressures were 4, 8, 15, 35, and 45 psf which correspond to Reynolds Numbers of 0.5×10^6, 0.7×10^6, 1.0×10^6, 1.5×10^6, and 1.7×10^6. The minimum Reynolds Number was limited by the ability to set and maintain a constant dynamic pressure in the test section. The maximum Reynolds Number was limited by

the loads imposed on the external balance system.

Standard two-dimensional buoyancy, solid blockage, and wake blockage corrections as described in Reference 8 were applied to the force and moment data.

Drag coefficient of the SM701 was also calculated by the momentum loss method. This method involves integrating the wake rake pressure data to obtain the section drag coefficient of the airfoil. The momentum loss method is very time consuming and was therefore run only on select cases. It was used to measure the laminar drag bucket of the airfoil, specifically from α = -6° to α = 6° in one degree increments at each Reynolds Number.

Extensive flow visualization was also performed on the SM701. The method used was white tempera paint and kerosene painted on the surface of the airfoil. The flow visualization was used to see laminar separation bubbles, transition, and separation.

TEST RESULTS

BASIC AIRFOIL

The basic SM701 airfoil was tested before aileron and turbulator modifications were made. This allowed a comparison with previous data, a baseline for future studies, and most importantly, the study of the airfoil performance at low Reynolds Numbers. Figures 10a-c show the Reynolds Number effects on lift, drag, and pitching moment coefficient. It can be seen that there is very little effect on the lift coefficient. C_{Lmax} is consistently about 1.53. The inverted stall is somewhat affected by Reynolds Number. The airfoil tends to stall at a more negative angle of attack as the Reynolds Number increases. The zero lift angle of attack is fairly consistent at -5.3 degrees. The positive stall is typically near 15 degrees angle of attack. The plot of momentum loss drag coefficient vs. lift coefficient shows a trend of decreasing drag with increasing Reynolds Number. The minimum drag typically occurs in the C_L = 0.3 to 0.5 range. The pitching moment coefficient also becomes more negative as the Reynolds Number is increased.

Comparisons of the current test data with the previous test data, as well as the predicted numerical data and experimental data obtained by Althaus at the Universitat Stuttgart[9] are made in Figures 11a-c. The angle of attack of the previous Texas A&M data has been shifted so the α_0 is the same for both sets of data. This change is to account for possible misalignment of the previous airfoil model. Examination of the lift coefficient comparison shows a 15% lower C_{Lmax} than numerically predicted. This value was also 6.3% lower than measured by Althaus. The current test measured a slightly higher C_{Lmax} than previously measured at Texas A&M. The negative stall was also measured at a more negative angle of attack. The zero lift angle of attack agreed very well with the numerically predicted and Althaus experimental data. A slight shift in the slope of the C_L curve is present in all the experimental data as compared to the predicted data. This slope change appears near zero degrees angle of attack. The measured momentum loss drag coefficient agrees well with the other experimental data, generally within 5%. Measured drag values were typically 18% higher than numerically predicted. The moment comparisons show the current measured data less negative than either Althaus or the predicted data but not as near zero as the previously measured Texas A&M data.

Flow visualization completed the data package on the baseline airfoil. Figures 12a-h show sample flow visualization photographs at the q = 15 psf, RN = 1 million condition. Flow is right to left on the upper surface photographs and left to right on the lower surface pictures. At α = -6°, the upper surface shows significant laminar flow. The lower surface shows transition very near the leading edge. A region of flow separation is visible starting about 90% chord.

The α = 0° case shows large amounts of laminar flow on both surfaces. Transition was observed at 55% on the upper surface and 45% on the lower surface. A smooth transition from laminar to turbulent flow is not evident in these photographs. The region where no flow appears on the surface is characteristic of a laminar separation bubble. No separation bubble was predicted numerically for this case however. Notice the two turbulent wedges caused by impurities in the flow visualization solution on the lower surface.

At α = 6° the transition location on the upper surface has moved forward to about 22%. Flow separation is visible at about 95% chord.

The lower surface shows nearly 60% laminar flow. About 12% laminar flow with separation occurring near 85% chord is present on the upper surface in the α = 10° case. Over 60% laminar flow is visible on the lower surface with no separation. The transition location at various angles of attack was determined by examining the photographs. In cases where laminar separation bubbles appeared present, transition location was taken as the forward most point of the bubble. Figure 13 compares the observed transition location with the numerically predicted locations. The observed locations were typically within 10% on both surfaces when compared with predicted results.

BASIC AIRFOIL WITH V-TAPE

Many sailplanes employ some form of turbulent drag reduction devices on lifting surfaces. Significant drag reductions have been measured by numerous researchers using a variety of techniques.[10] Among the drag reduction devices used on sailplanes is V-tape turbulators. The V-tape used in this study was made by sticking two layers of 0.5 inch wide Labeling Tape together, then cutting in half with pinking shears (Figure 14). This device was 0.02 inches high, approximately 0.25 inches wide, and spanned the airfoil.

The tape was applied to the basic airfoil at four separate locations: 80%, 63%, and 45% chord on the lower surface and 12% chord on the upper surface (Figure 15). External balance data was acquired through positive and negative stall at three or four Reynolds Numbers for each V-tape location and momentum loss method drag coefficients were obtained for the lower surface V-tape locations at RN = 1 million. Note the external balance drag values measured are not strictly two-dimensional due to corner effects at the airfoil/tunnel junctures. The data should be used for comparison and not absolute values. Figures 16a-c show the Reynolds Number effects on the data with V-tape at 63% chord. It can be seen there is a slight increase in C_{Lmax} at the lowest Reynolds Number case. The inverted C_{Lmax} curve is essentially unchanged from the basic airfoil. No shift in the α_0 was observed. The drag again decreased and the pitching moment became more negative with increasing Reynolds Number.

Figures 17a-d compare the V-tape location results with the basic airfoil at a constant Reynolds Number of 1 million. Very little change in any portion of the lift curve is evident for any V-tape location on the lower surface. The runs with V-tape on the airfoil upper surface show a loss in C_{Lmax} and a shift in the α_0 angle to the right of approximately 0.65 degrees. The external balance drag coefficient results show a very slight drag decrease with the addition of the V-tape on the lower surface. A significant increase was observed with the tape on the upper surface. The pitching moment coefficient data again shows very little effect with the V-tape on the lower surface. The upper surface V-tape did make the pitching moment coefficient approximately 13% less negative through much of the α range. The momentum loss drag coefficients show a general decrease in drag with all lower surface V-tape locations for C_L's below 0.5. For higher C_L's the drag tended to be larger than the clean configuration. The V-tape located at 80% chord tended to be the best position tested, and the 45% chord location was the worst. Momentum loss method data was not obtained on the 12% upper surface configuration.

Flow visualization was also performed on the 63% V-tape location. Examination of flow visualization photographs from α = -6° through α = 3° show the transition location to be forward of the V-tape location. Figures 18a-c show the flow on the lower surface at α = 6, 10, and 15 degrees respectively. The α = 6° photo shows the transition location slightly forward of the V-tape. The α = 10° and α = 15° photos show transition caused by the V-tape. No separated flow is visible aft of the V-tape.

AIRFOIL WITH AILERON

The World Class Glider Technical Specifications require an unflapped airfoil; the SM701 was specifically designed with this constraint in mind. It is believed however, sailplane designers wishing to employ the SM701 would use ailerons for control. A twenty-five percent aileron was suggested by the airfoil designers. Aileron deflections runs were made at five different angle settings: -20, -10, 0, 10, and 20 degrees.

Initial comparisons between the airfoil without an aileron and the airfoil with the

aileron at 0 degrees were made. Figures 19a-c show the lift, drag, and moment coefficient results as compared to the clean airfoil. It can be seen the aileron has no effect on either positive or negative stall values for C_L. A slight shift of the curve to the right is evident. The C_D curve shows a significant increase in drag with the aileron. The airfoil with aileron typically has 10% higher drag than the clean airfoil through the moderate C_L range. The C_m curve also shows slightly more negative C_m at positive angles of attack and slightly less negative C_m at negative angles of attack. The C_m data repeats quite well at $\alpha = 0°$. These changes suggest a drag increase is occurring at the aileron cut on the lower surface.

The aileron deflection comparisons can be seen in Figures 20a-c. The C_L curves show an increase in $C_{L\,max}$ with positive aileron deflection and an increase in α_0 with an increase in negative aileron deflection. The curves tend to shift as expected, except for the ±20 degree cases near α_0. The C_D curves tend to follow the expected trends, except again at ±20 degree aileron deflection cases. Here flow separation is clearly present and significant drag increases are seen. The C_m curves show a more negative C_m with positive aileron deflection and a less negative or even positive C_m with negative aileron deflections.

CONCLUSIONS

The results of a two-dimensional 16 inch chord SM701 airfoil wind tunnel test through the 500,000 to 1.7 million Reynolds Number range have been reported. Comparisons were made with numerically predicted and previously obtained wind tunnel data. The effects of V-tape for use in turbulent drag reduction on the airfoil were studied. Experiments were also performed to study the effects of aileron deflection. Six component external balance data, momentum loss method drag data, and flow visualization photographs were obtained.

Performance trends of the basic airfoil were verified. The C_{Lmax} was measured to be 1.53 which is 15% lower than predicted. The zero lift angle of attack was verified to be -5.3°. The drag coefficient was measured 18% higher than predicted, but within 5% of other experimental data. Transition locations were typically observed within 10% of predicted values through flow visualization.

The V-tape studies showed slight performance gains by using the tape on the lower surface. Significant losses were observed by placing V-tape on the upper surface. The results suggest a small benefit through the low C_L range from using V-tape located at 80% chord on the lower surface of the SM701.

Addition of the aileron to the basic airfoil had little effect on the lift coefficient for an aileron deflection of 0°. The drag was increased by about 10%. The ±20° deflections did tend to be a bit extreme in that the curves significantly changed shape due to separated flows. Deflections less than ±20° showed curve shifts as expected.

ACKNOWLEDGMENTS

Grateful acknowledgment is extended to all the people at the NASA Langley Research Center who provided consultation and support throughout the project. The authors would like to extend a special thank-you to Mr. Danny Schulz of the TAMU-LSWT for his considerable help in design and construction of the model used in these studies.

REFERENCES

1. Morelli, Piero: The "World Class" Glider Design Competition. FAI Announcement. Technical Specifications, November, 1990.
2. Somers, Dan M.; and Maughmer, Mark D.: The SM701 Airfoil. Airfoils Incorporated, State College, Pennsylvania, 1990. (also Somers, Dan M.; and Maughmer, Mark D.: The SM701 Airfoil: An Airfoil for World Class Sailplanes. Technical Soaring, vol. 16, no. 3, July 1992, pp. 70-77.)
3. Nicks, Oran; Steen, Gregory; Heffner, Michael; and Bauer, David: Wind Tunnel Investigation and Analysis of the SM701 Airfoil. Presented at the XXII OSTIV Congress, August, 1991.
4. Korkan, Kenneth D.; Griffiths, Robert C.; and Uellenberg, Stefan A.: Verification of the SM701 Airfoil Aerodynamic Characteristics Utilizing Theoretical Techniques. Presented at the XXII OSTIV Congress, August, 1991.

5. Low Speed Wind Tunnel Facility Handbook. Texas A&M University, College Station, Texas, 1985.
6. Hafermalz, Scott; and Steen, Gregory: Freestream Turbulence Intensity Measurements in the Texas A&M University Low Speed Wind Tunnel. Texas A&M University, July, 1992.
7. Kline, S.J.; and McClintock, F.A.: Describing Uncertainties in Single-Sample Experiments. Mechanical Engineering, vol. 75, no. 1, January 1953, pp. 3-8.
8. Rae, William H.; and Pope, Alan: Low Speed Wind Tunnel Testing. John Wiley and Sons, New York, 1984.
9. Althaus, D.; and Wurz, W.: Wind Tunnel Tests of the SM701 Airfoil. Universitat Stuttgart, 1991.
10. Lin, J.C.; Howard, F.G.; Bushnell, D.M.; and Selby, G.V.: Comparative Study of Control Techniques for Two-Dimensional Low-Speed Turbulent Flow Separation. Presented at the IUTAM Symposium on Separated Flows and Jets, July, 1990.

TAMU–LSWT Facility Diagram

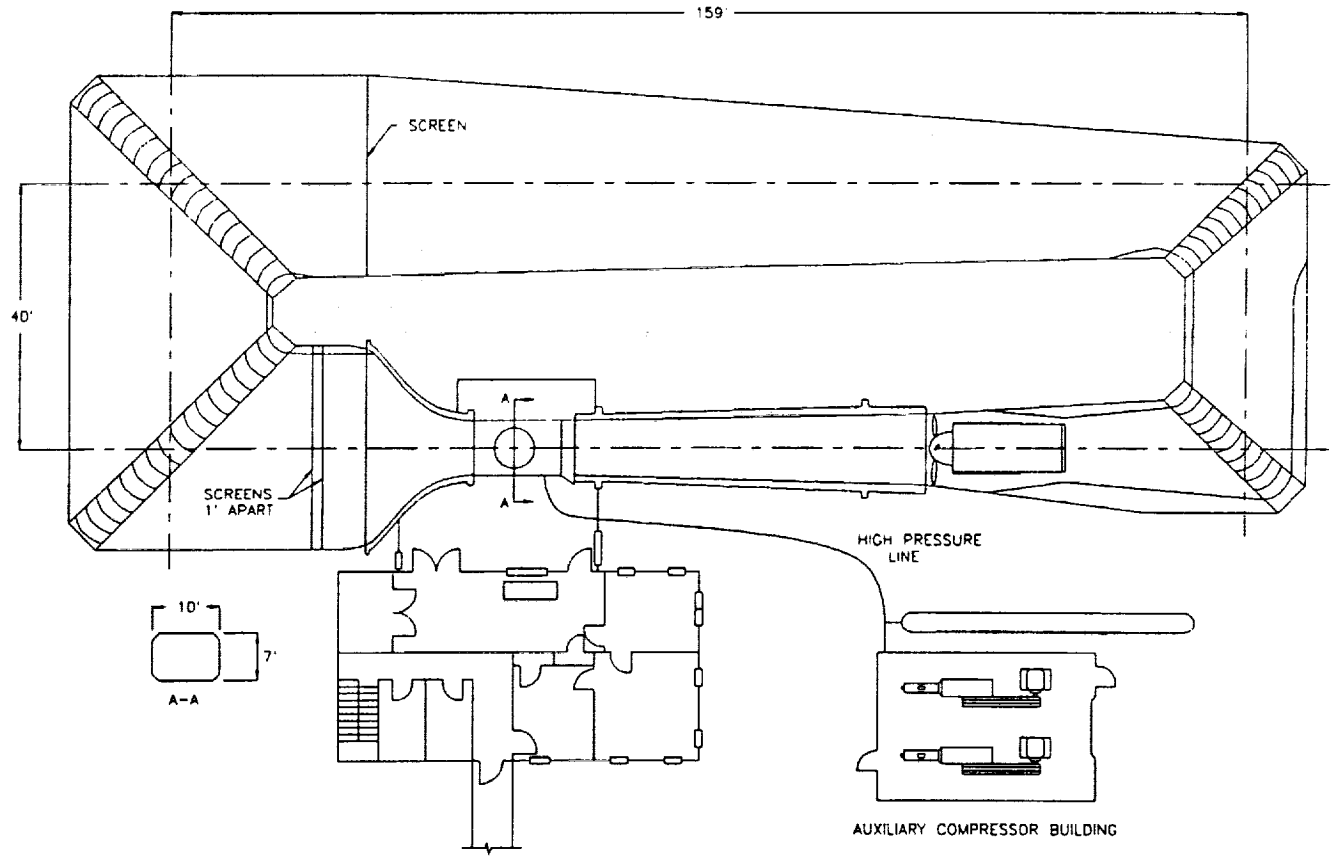

Figure 1 - TAMU-LSWT Facility Diagram

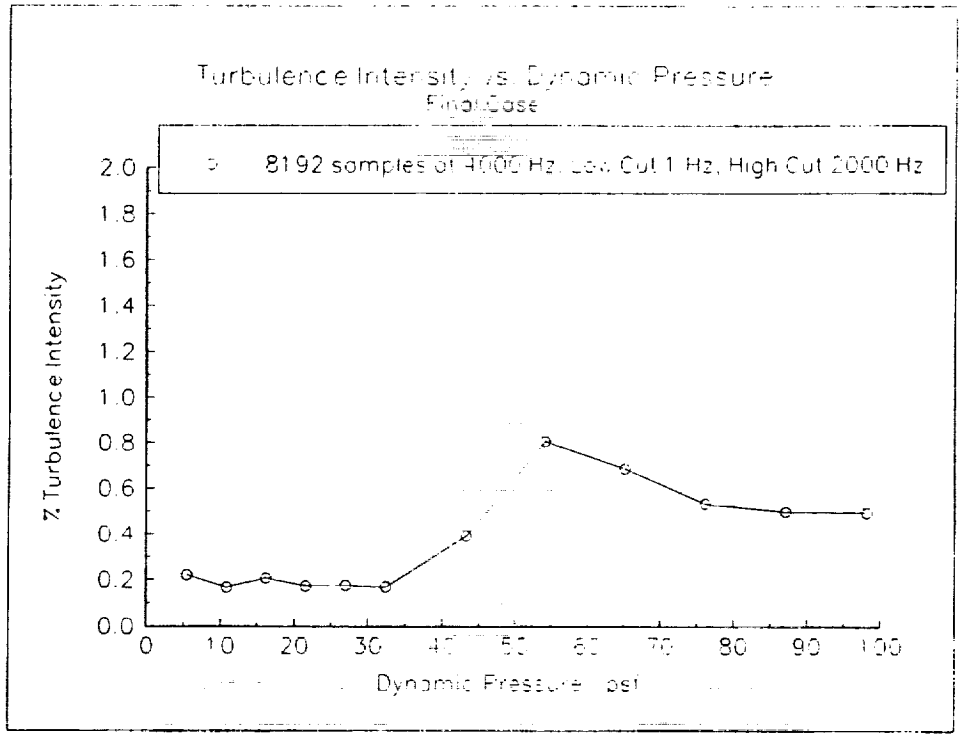

Figure 2 - Freestream Turbulence Intensity Levels

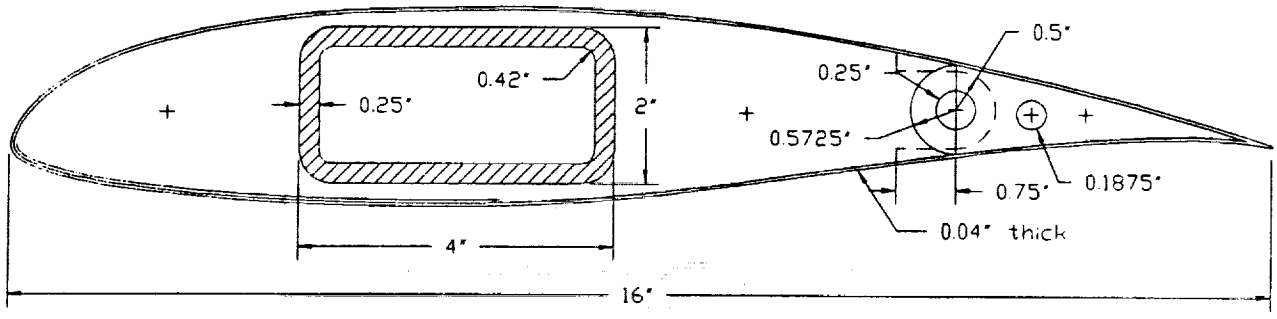

**NOTE: All circle dimensions are radius dimensions

Figure 3a - TAMU-LSWT SM701 Model Cross Section Before Aileron Cut

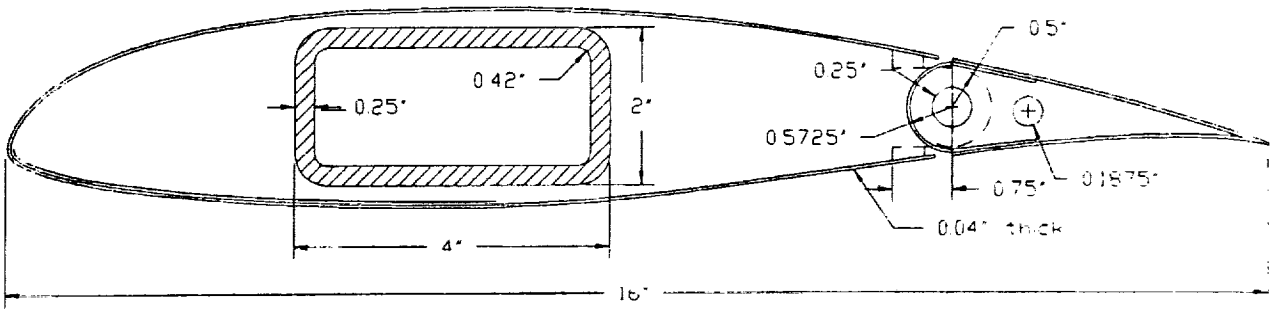

Figure 3b - TAMU-LSWT SM701 Model Cross Section After Aileron Cut

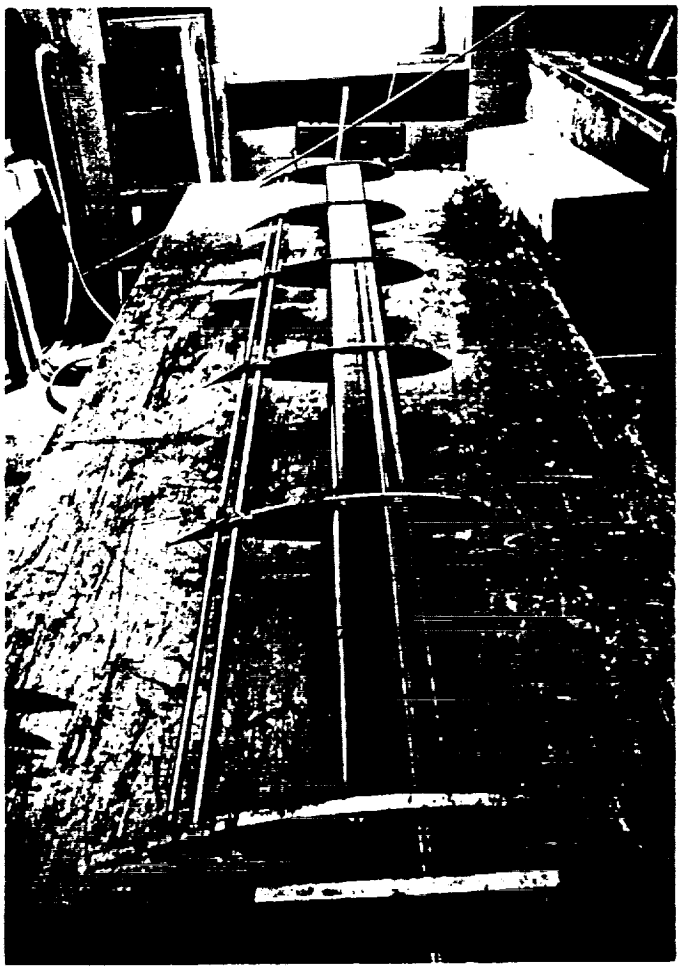

Figure 4 - Model Support Structure

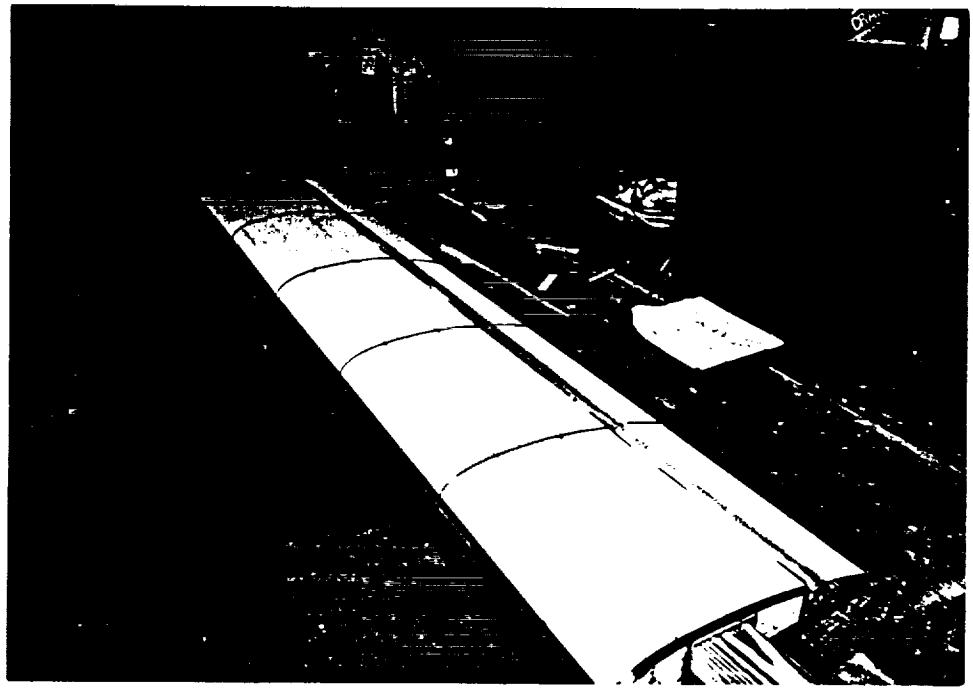

Figure 5 - Foam Sanded to Shape Before Fiberglass Application

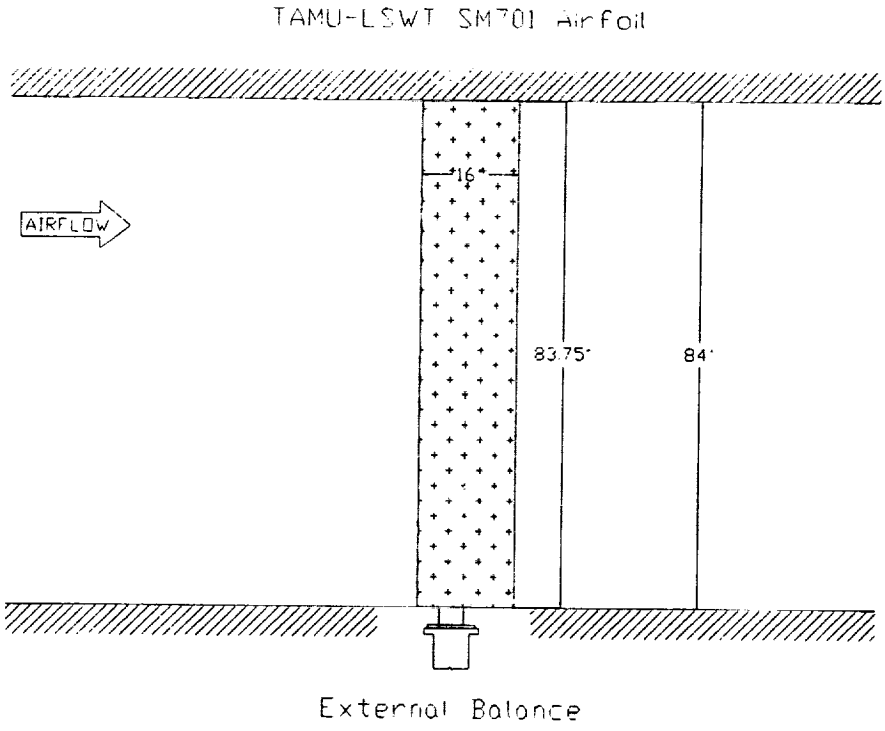

Figure 6 - Line Drawing of SM701 Airfoil in TAMU-LSWT Test Section

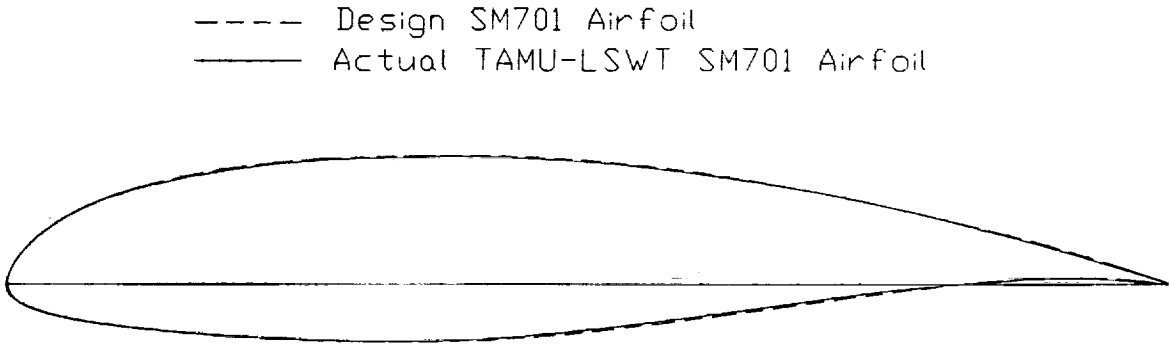

Figure 7 - Design and Actual SM701 Shape Comparison

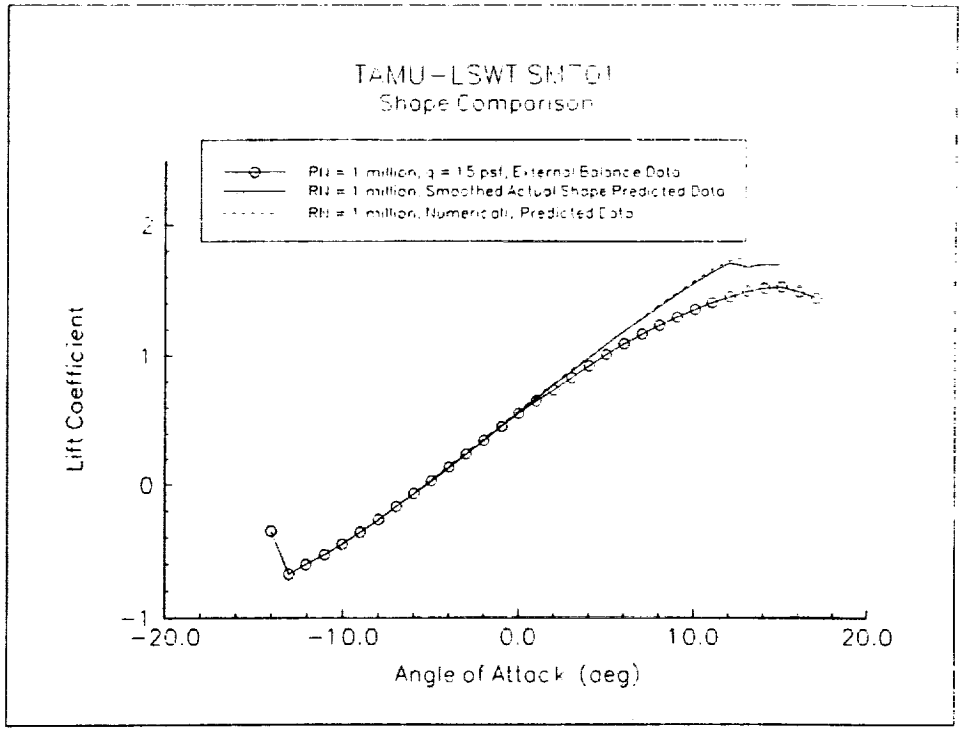

Figure 8a - Model and Desired Shape Comparison on Lift Coefficient (RN = 1 million)

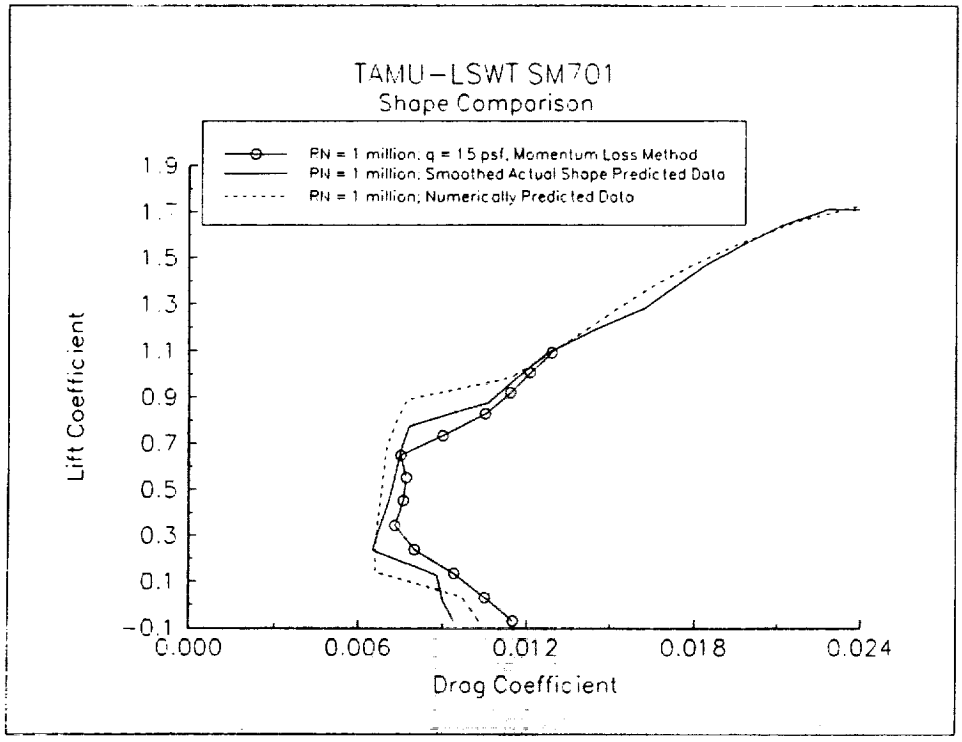

Figure 8b - Model and Desired Shape Comparison on Drag Coefficient (RN = 1 million)

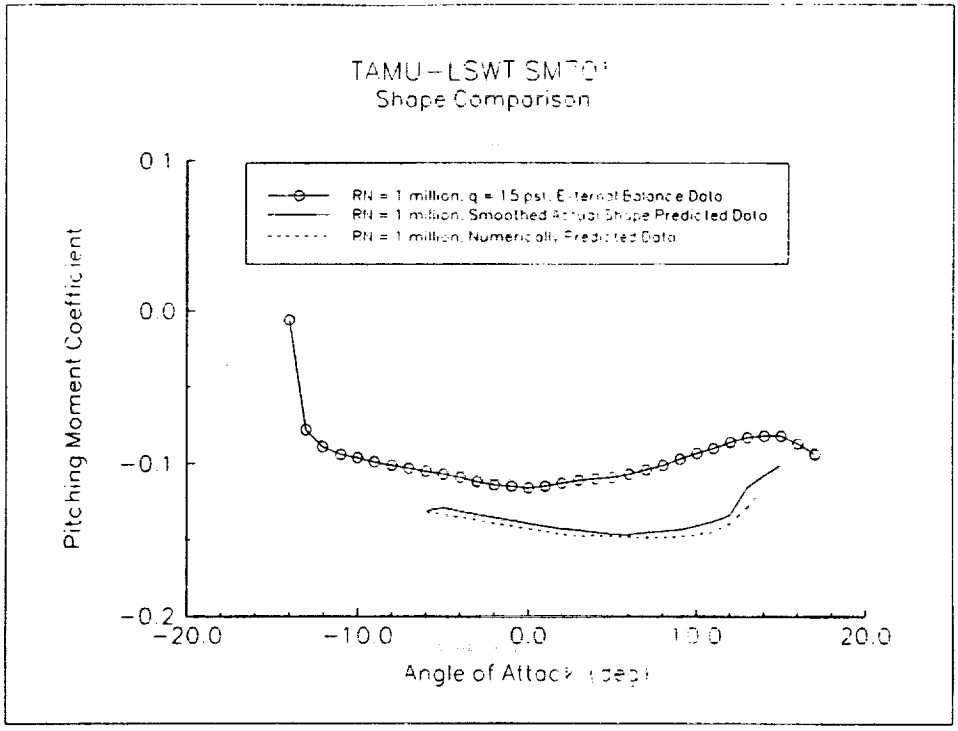

Figure 8c - Model and Desired Shape Comparison on Moment Coefficient (RN = 1 million)

RN (10^6)	q_{set} (psf)	Wq_{act} (psf)	WC_L	$WC_{D_{bal}}$	WC_m	$WC_{D_{mom}}$
0.5	4	0.2187	0.0286	0.0056	0.0079	0.00109
0.7	8	0.2190	0.0151	0.0028	0.0040	0.00056
1.0	15	0.2195	0.0085	0.0015	0.0022	0.00030
1.5	35	0.2210	0.0047	0.0006	0.0012	0.00013
1.7	45	0.2217	0.0042	0.0005	0.0010	0.00010

Table 1 - Calculated Uncertainty Results in Measured Readings at $\alpha = 0°$

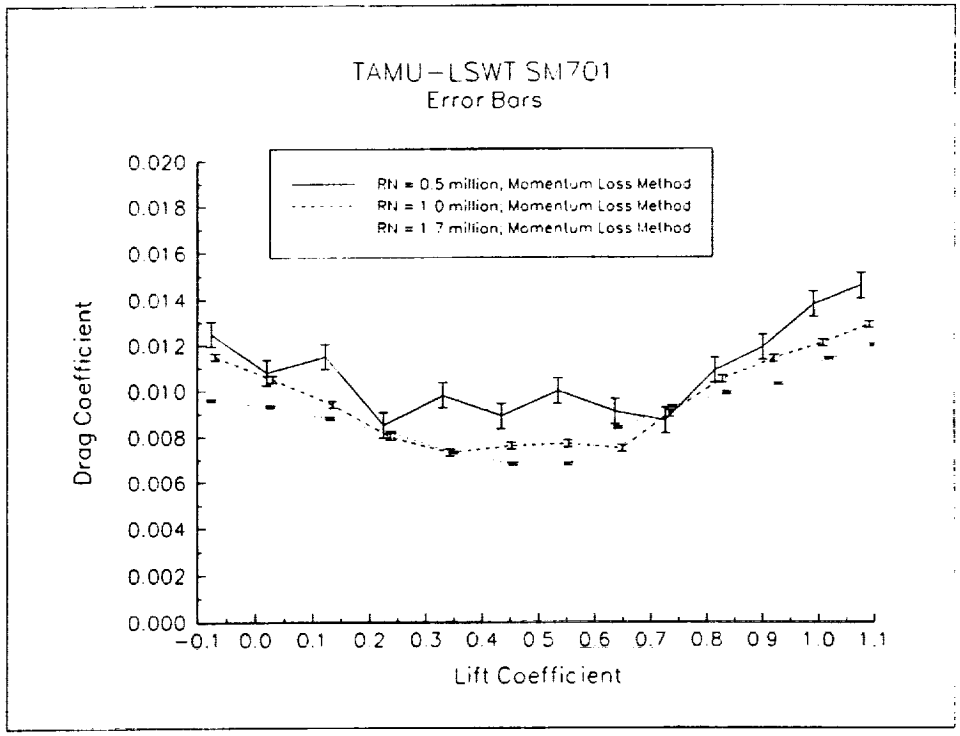

Figure 9 - Momentum Loss Drag Coefficient with Error Bars

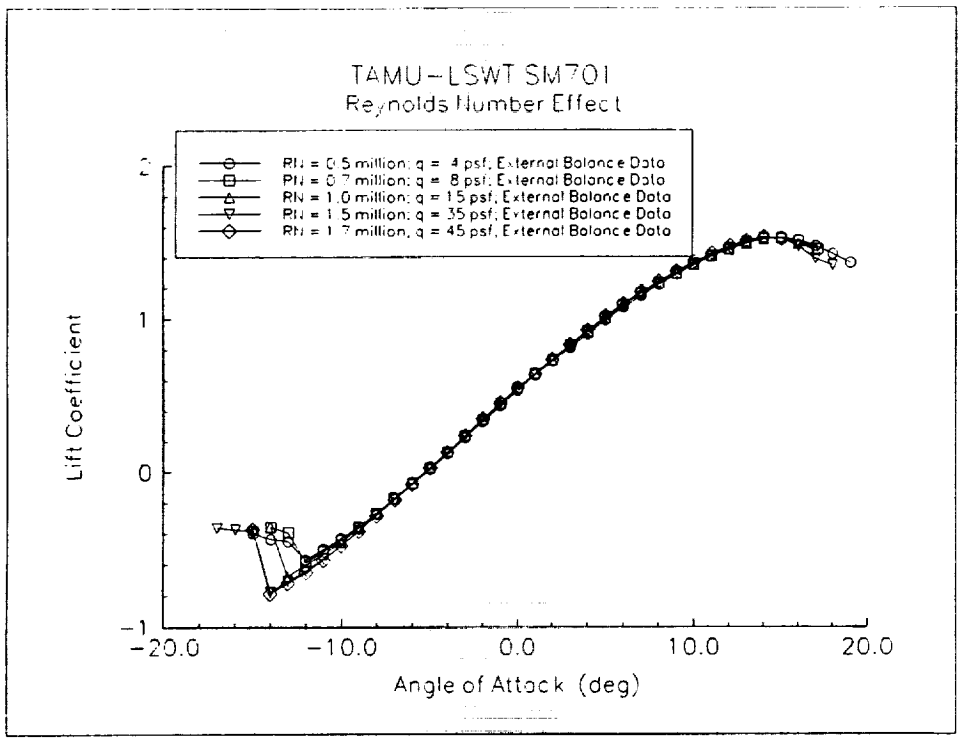

Figure 10a - Reynolds Number Effect on Lift Coefficient

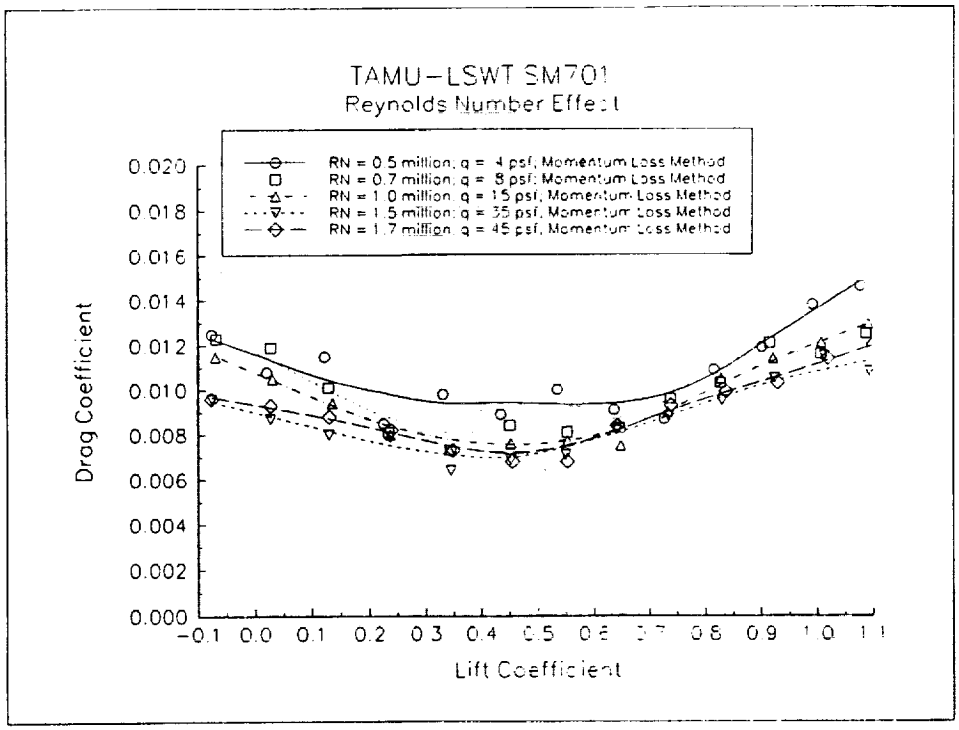

Figure 10b - Reynolds Number Effect on Momentum Loss Drag Coefficient

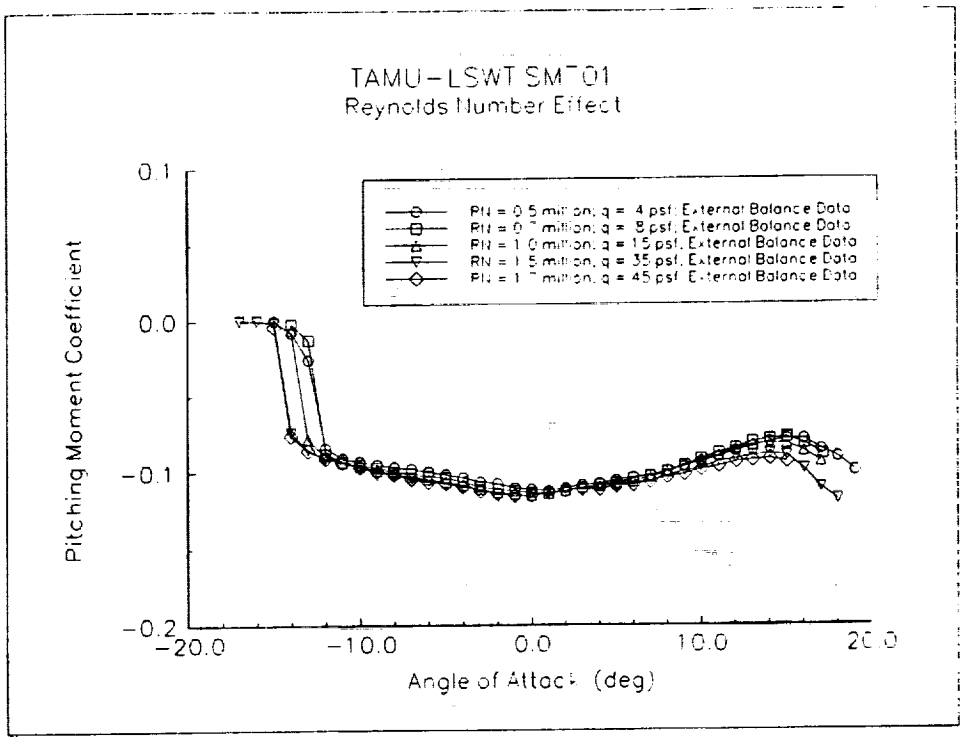

Figure 10c - Reynolds Number Effect on Pitching Moment Coefficient

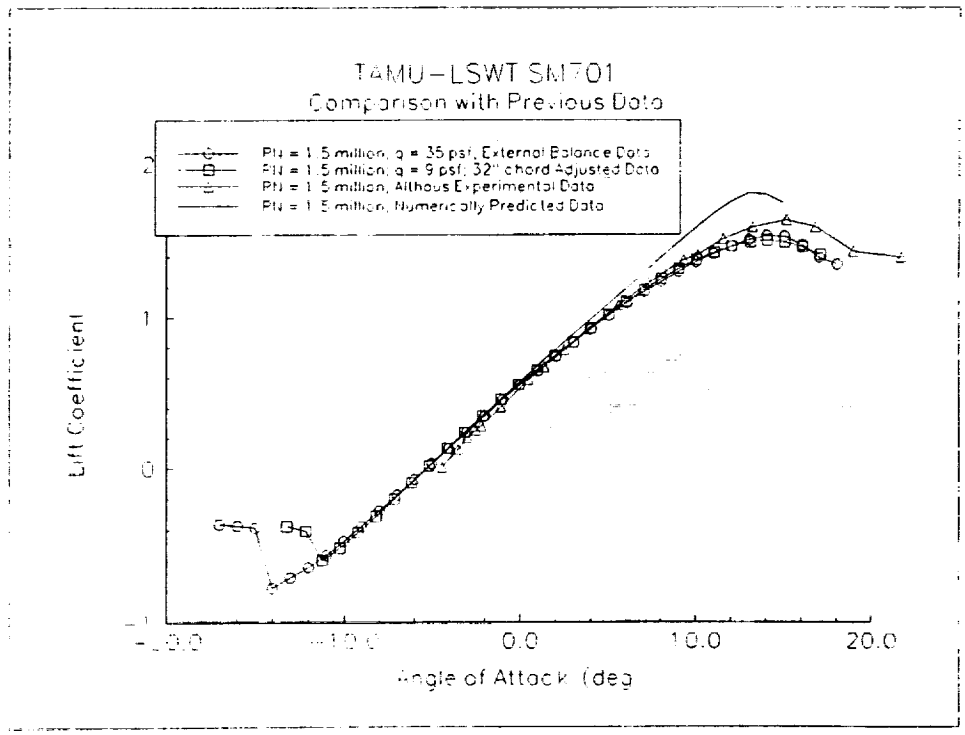

Figure 11a - Lift Coefficient Comparison

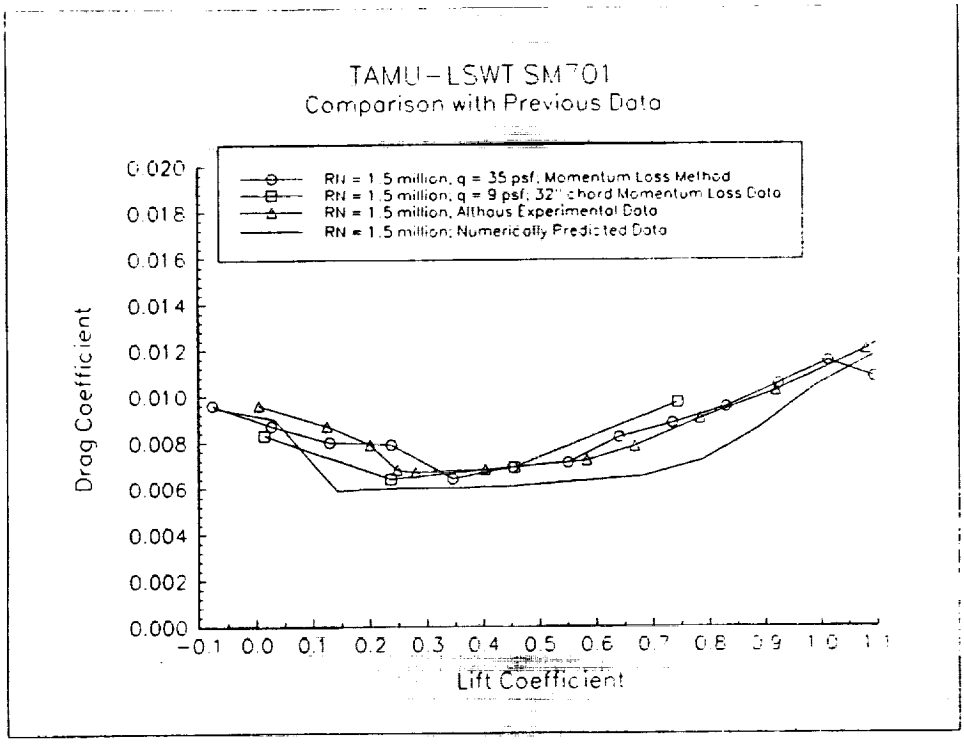

Figure 11b - Drag Coefficient Comparison

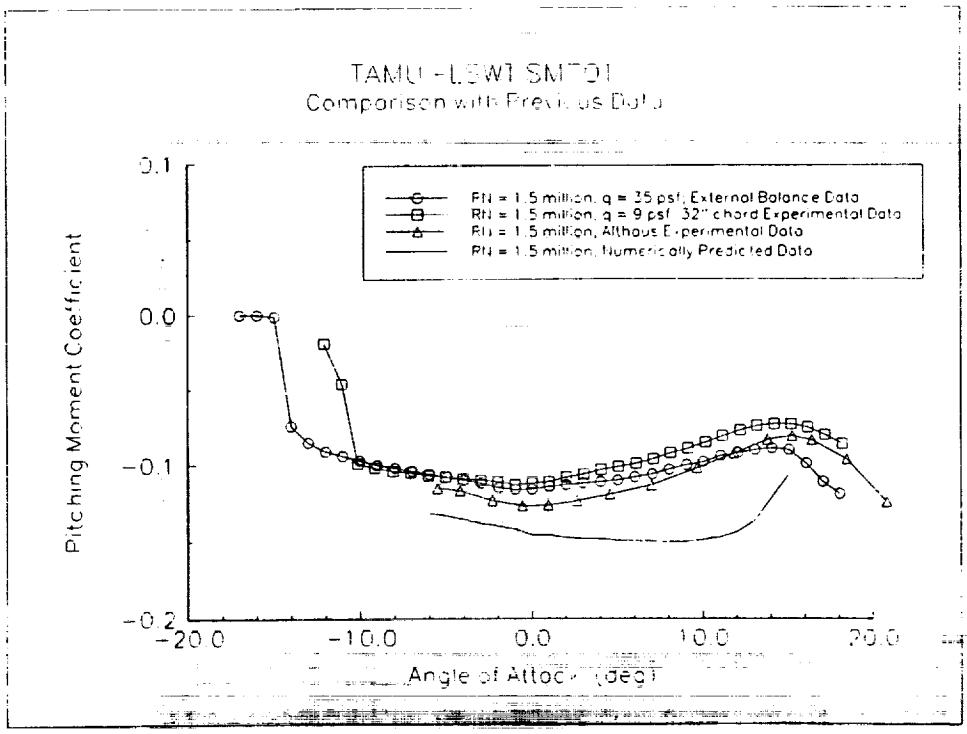

Figure 11c - Pitching Moment Coefficient Comparison

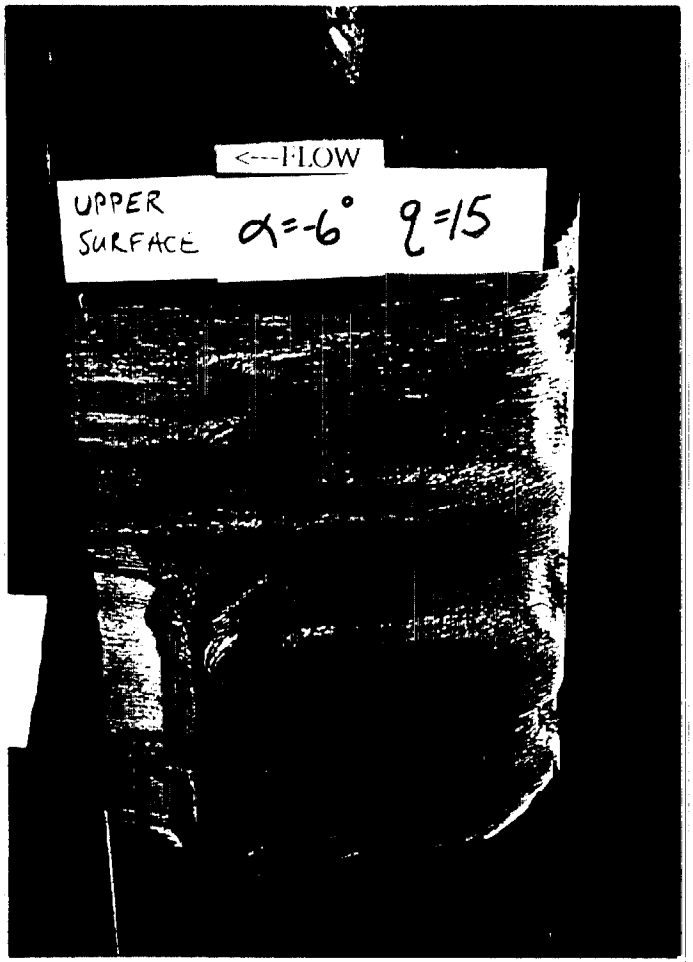

(a) α = -6°, upper surface

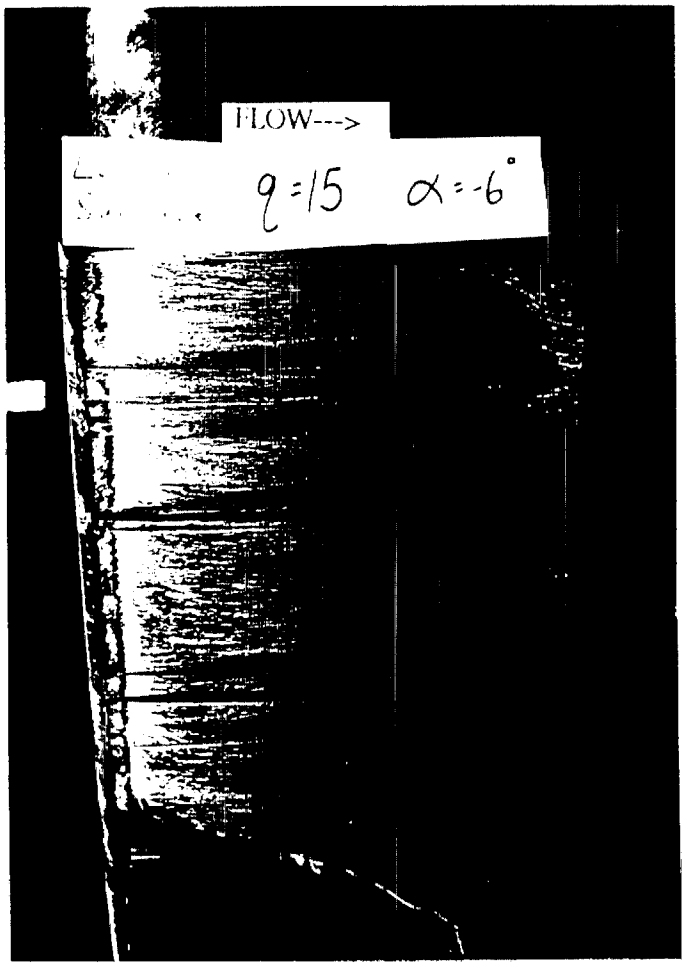

(b) α = -6°, lower surface

Figure 12 - Flow Visualization Photographs (q = 15 psf, RN = 1 million)

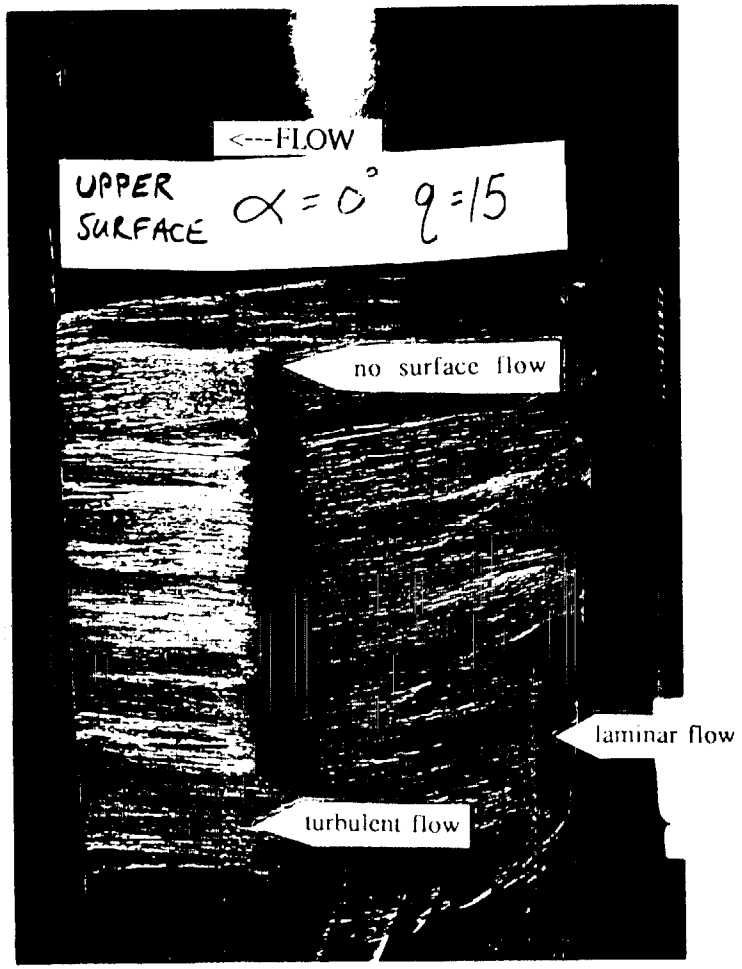

(c) α = 0°, upper surface

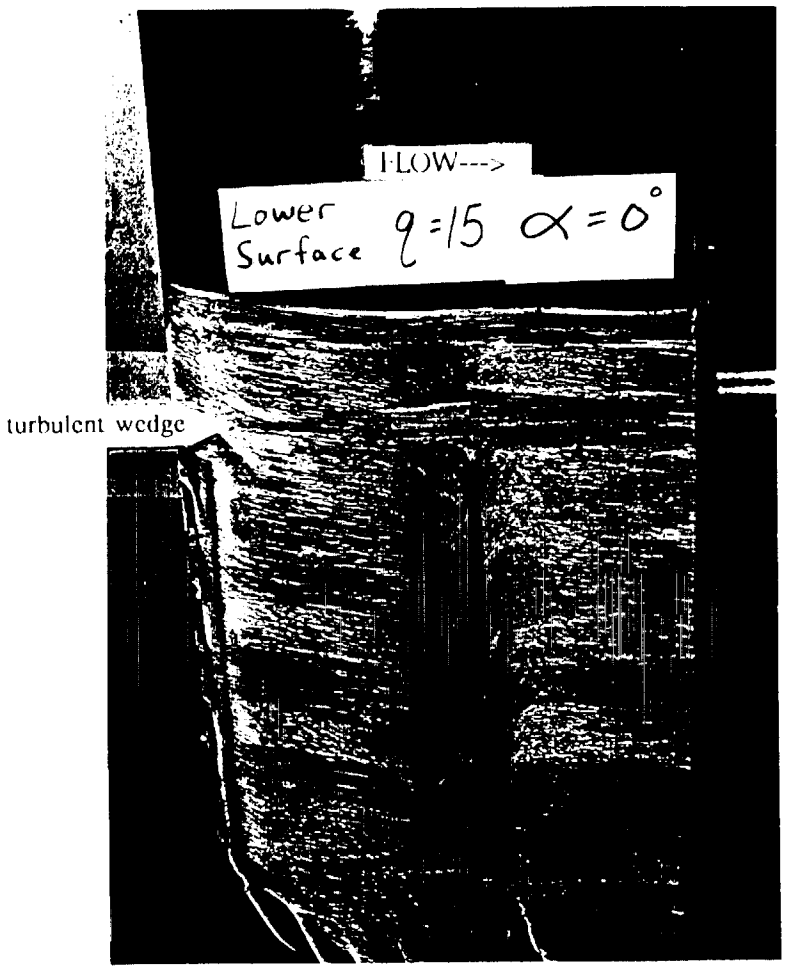

(d) α = 0°, lower surface

Figure 12 - Flow Visualization Photographs (q = 15 psf, RN = 1 million)

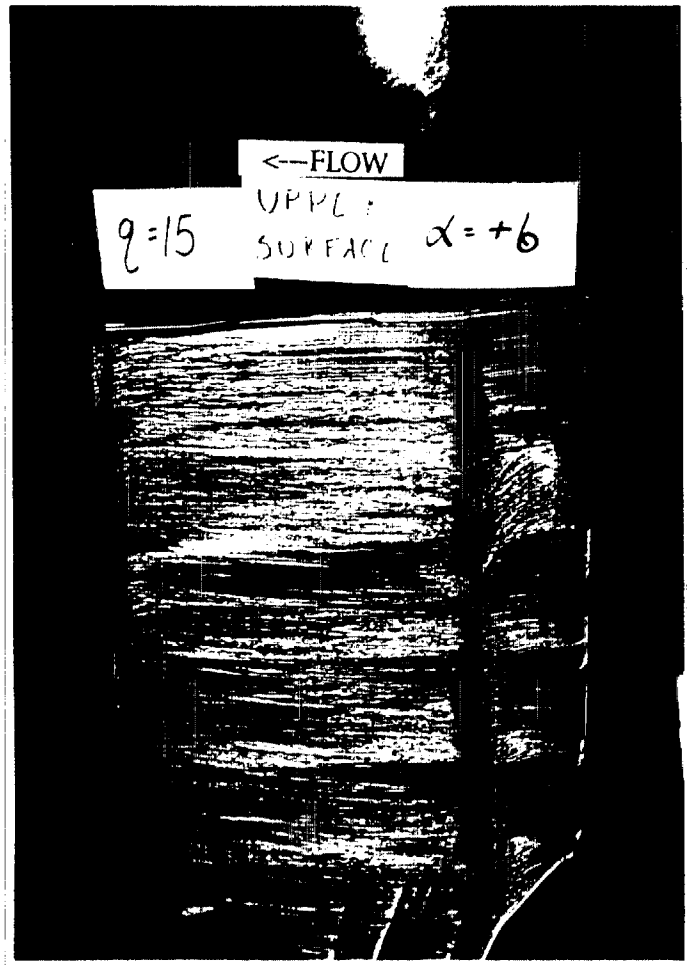

(c) α = 6°, upper surface

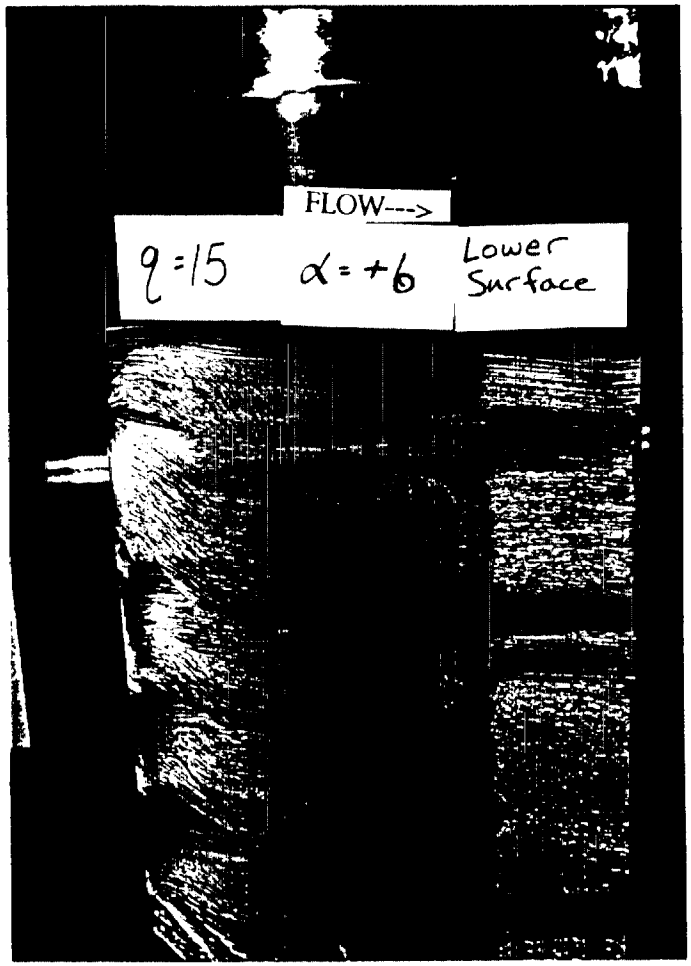

(f) α = 6°, lower surface

Figure 12 - Flow Visualization Photographs (q = 15 psf, RN = 1 million)

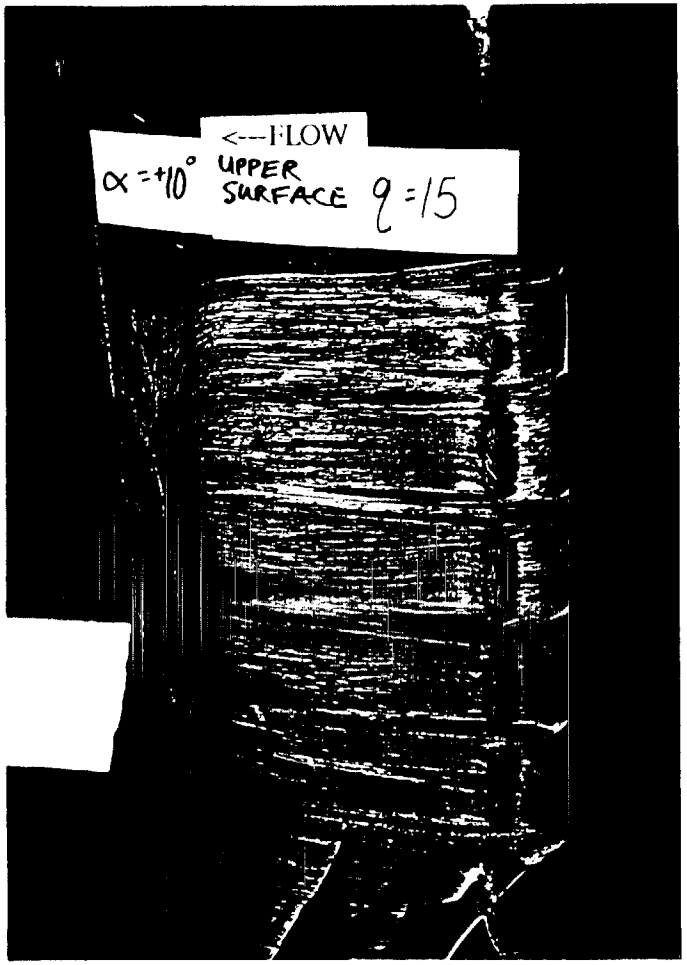

(g) α = 10°, upper surface

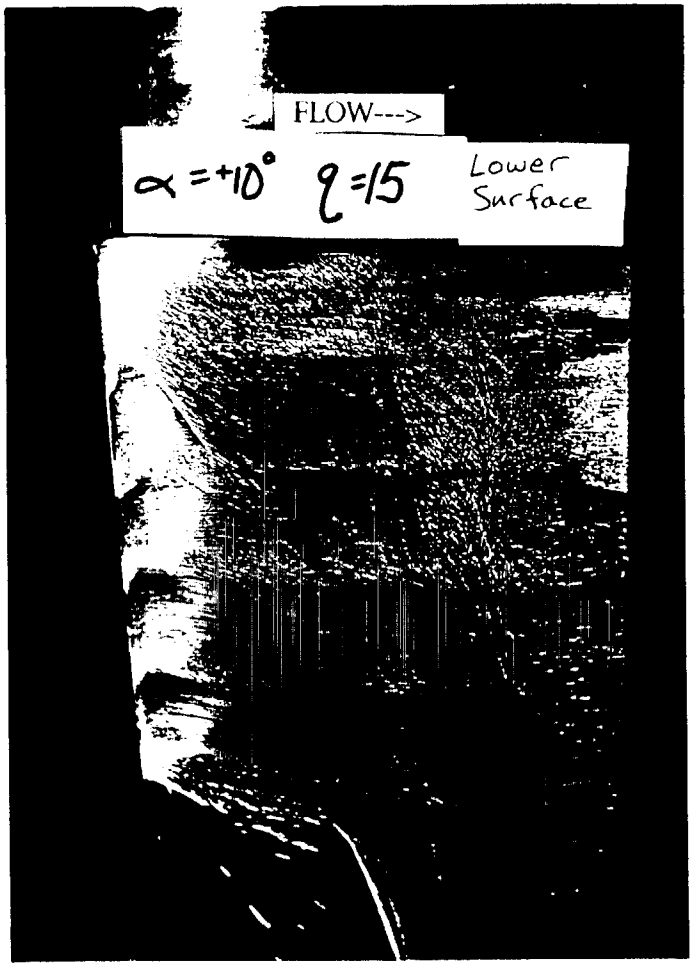

(h) α = 10°, lower surface

Figure 12 - Flow Visualization Photographs (q = 15 psf, RN = 1 million)

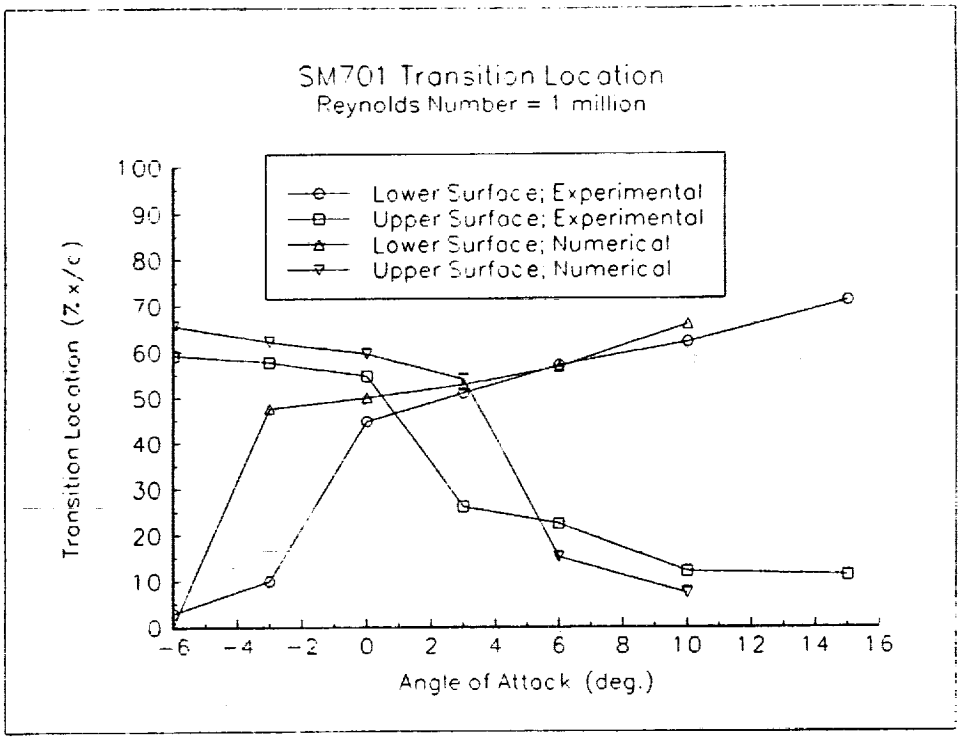

Figure 13 - Transition Location Comparison (RN = 1 million)

Figure 14 - V-Tape Sample

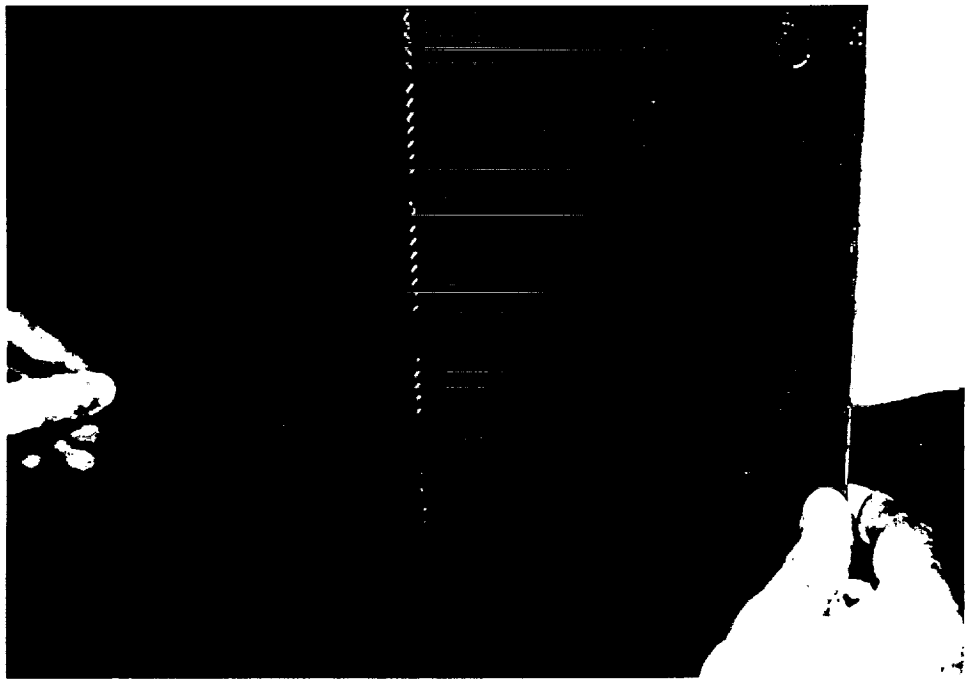

Figure 15 - V-Tape Placement on Airfoil

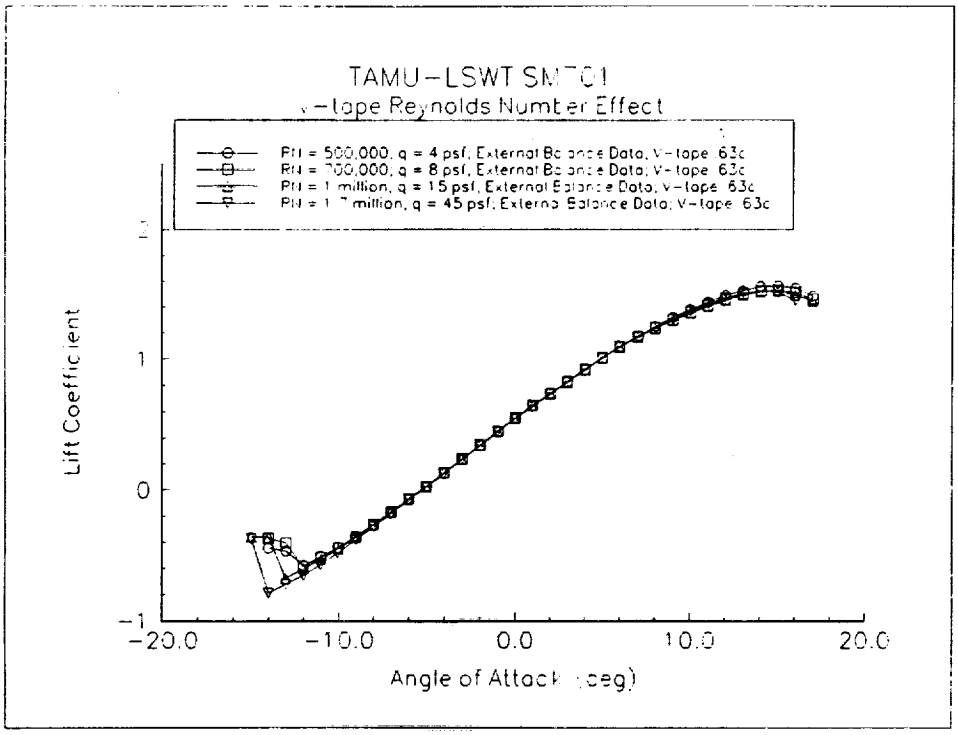

Figure 16a - V-Tape Reynolds Number Effect on Lift Coefficient

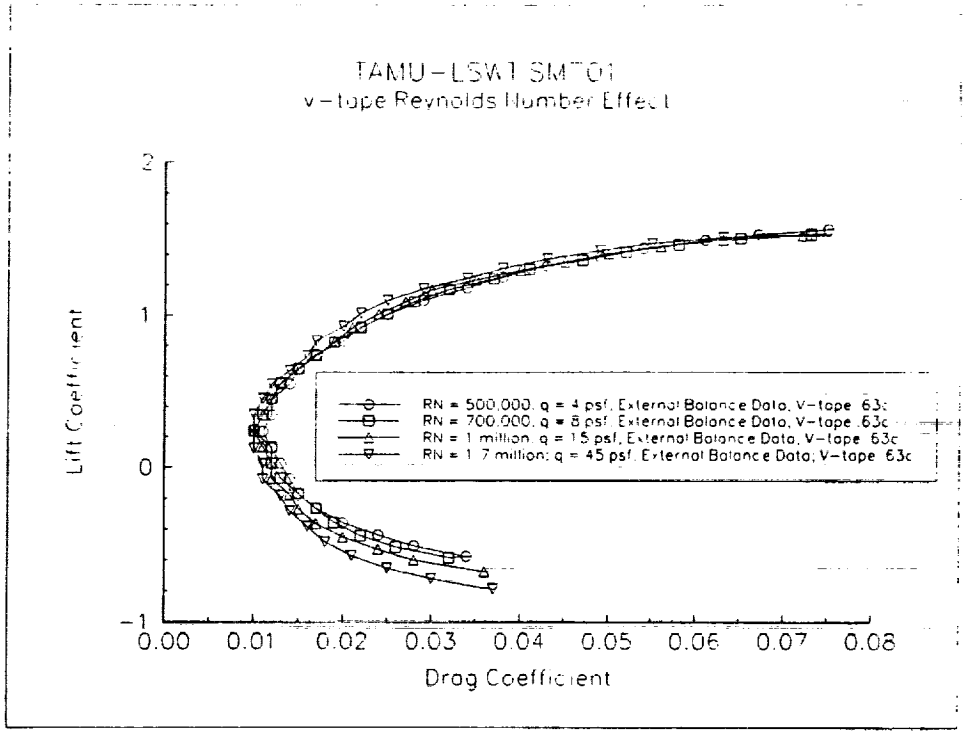

Figure 16b - V-Tape Reynolds Number Effect on Drag Coefficient

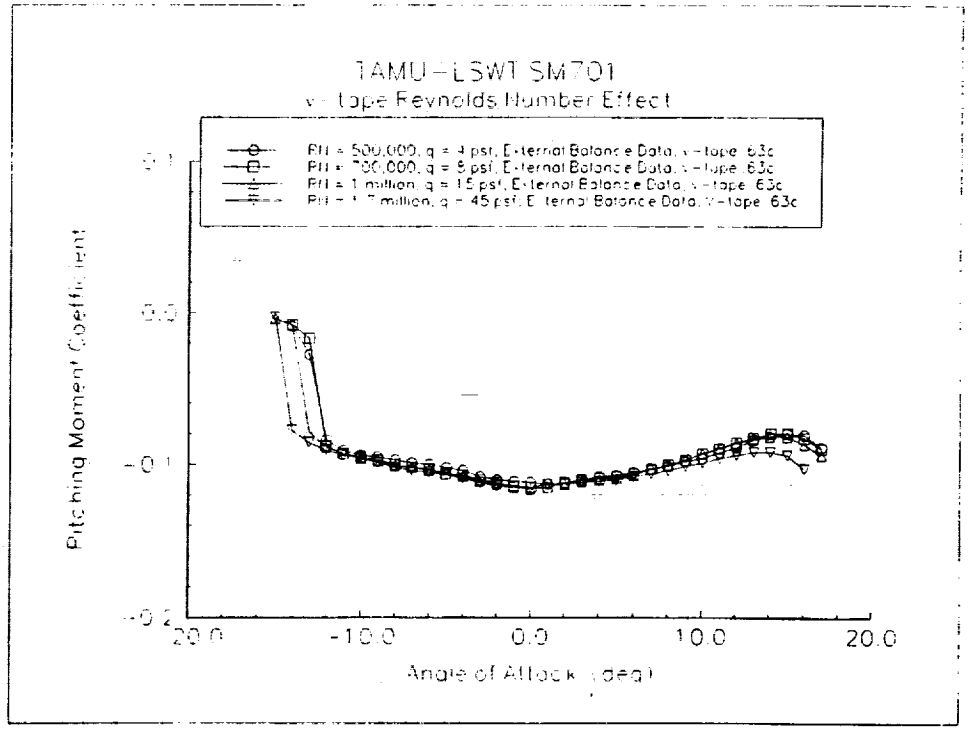

Figure 16c - V-Tape Reynolds Number Effect on Pitching Moment Coefficient

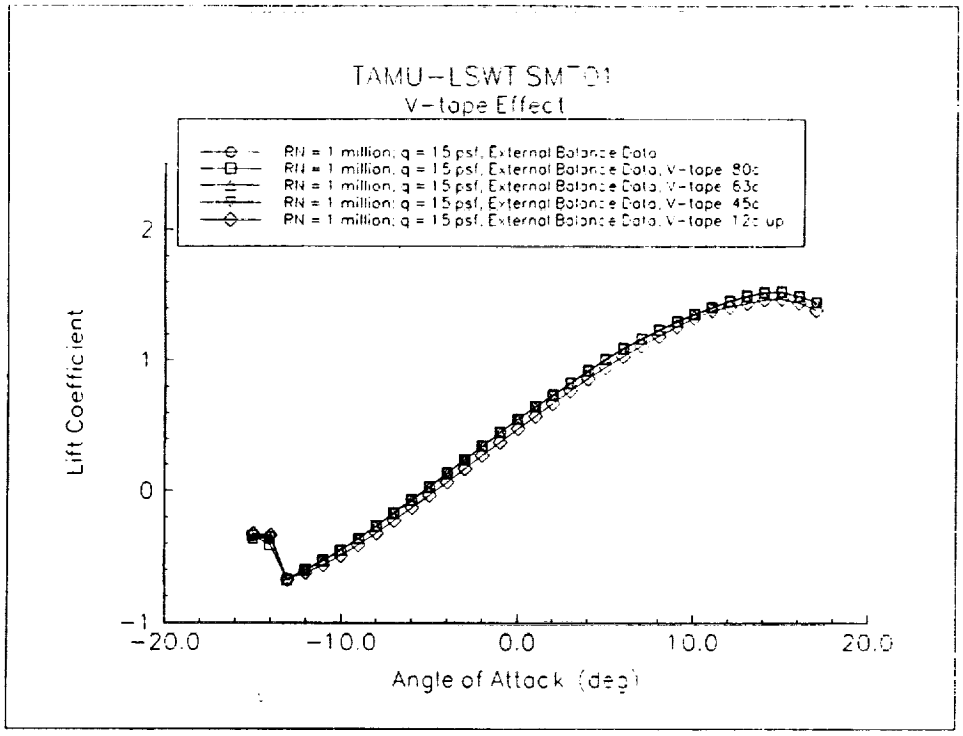

Figure 17a - V-Tape Effect on Lift Coefficient (RN = 1 million)

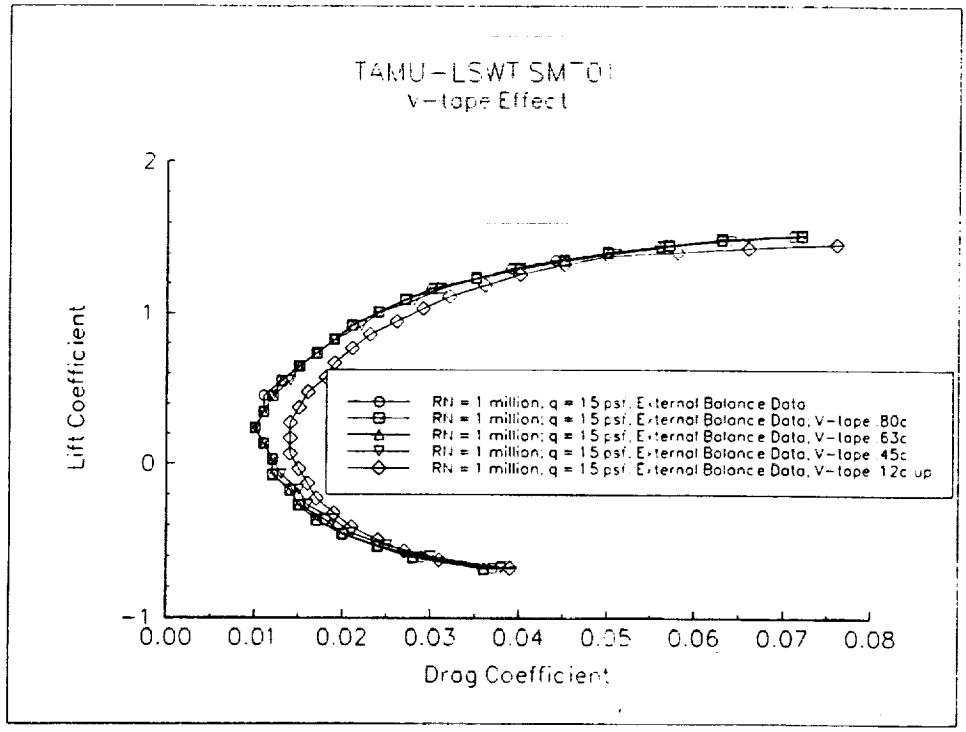

Figure 17b - V-Tape Effect on External Balance Drag Coefficient (RN = 1 million)

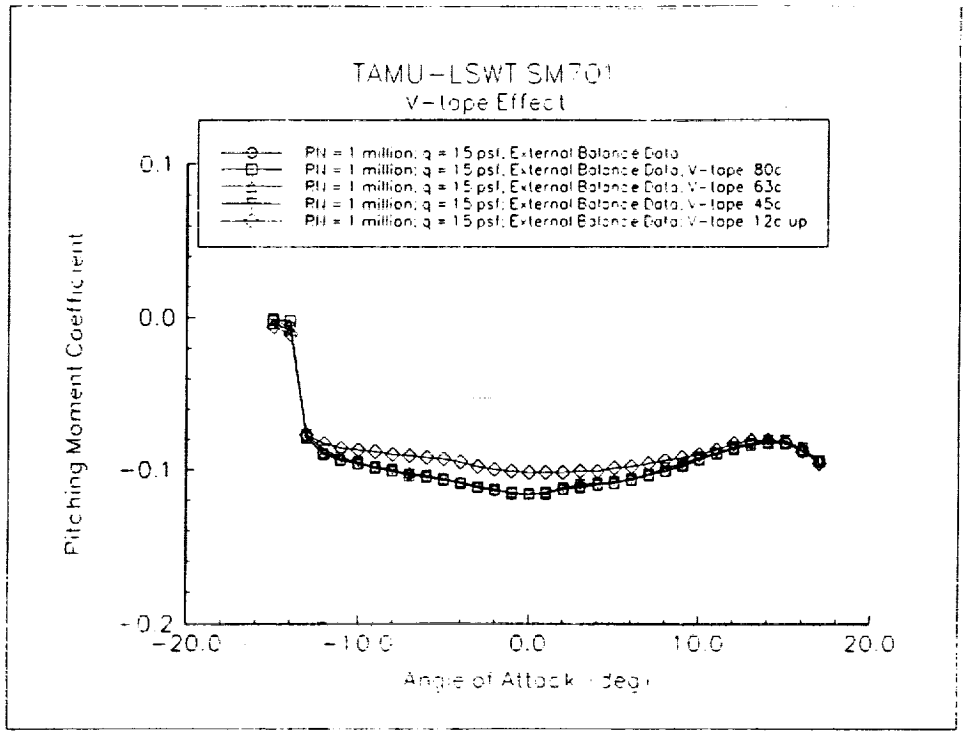

Figure 17c - V-Tape Effect on Pitching Moment Coefficient (RN = 1 million)

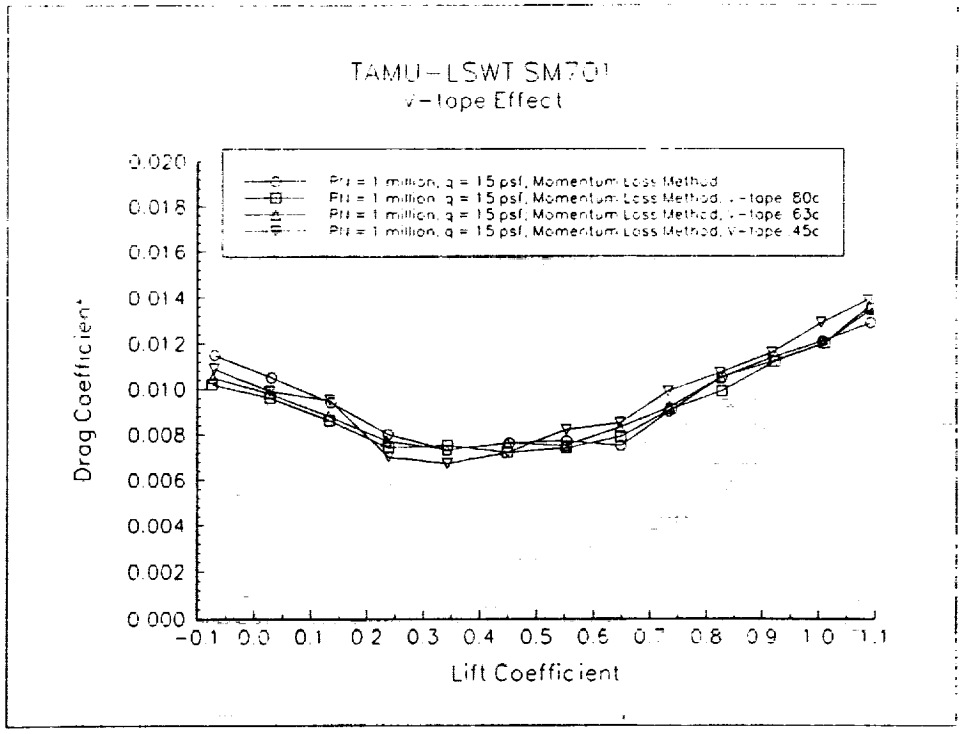

Figure 17d - V-Tape Effect on Momentum Loss Drag Coefficient (RN = 1 million)

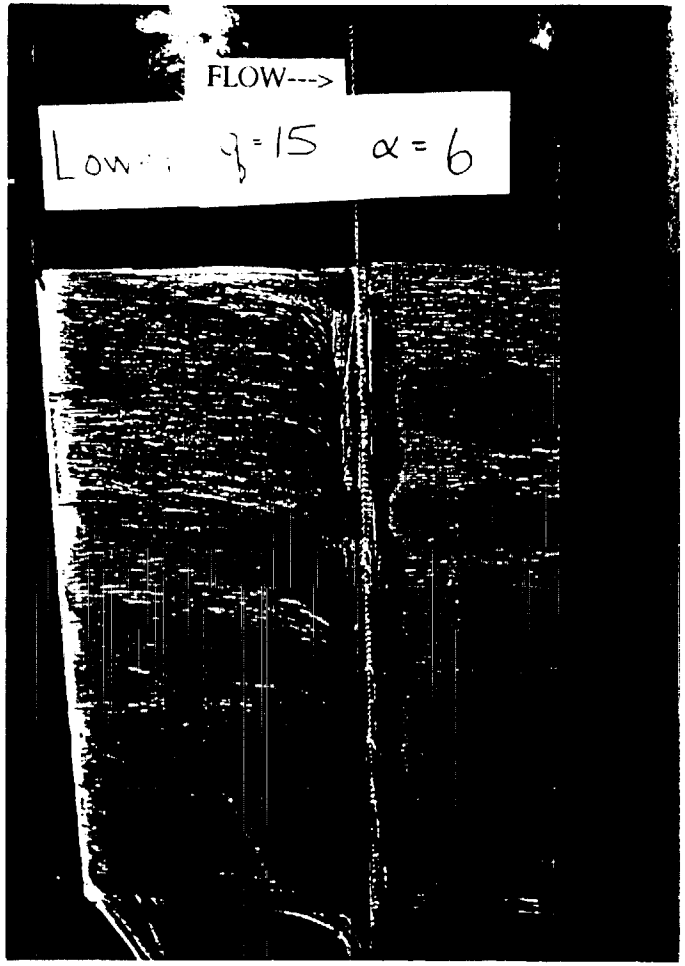

(a) $\alpha = 6°$

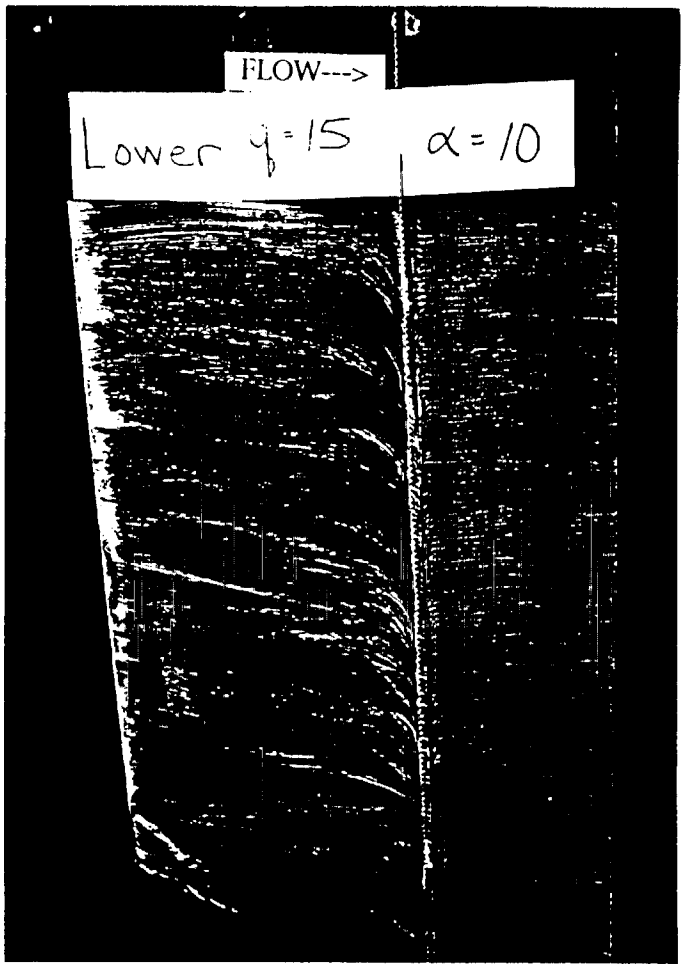

(b) $\alpha = 10°$

Figure 18 - V-Tape Lower Surface Flow Visualization Photographs (RN = 1 million)

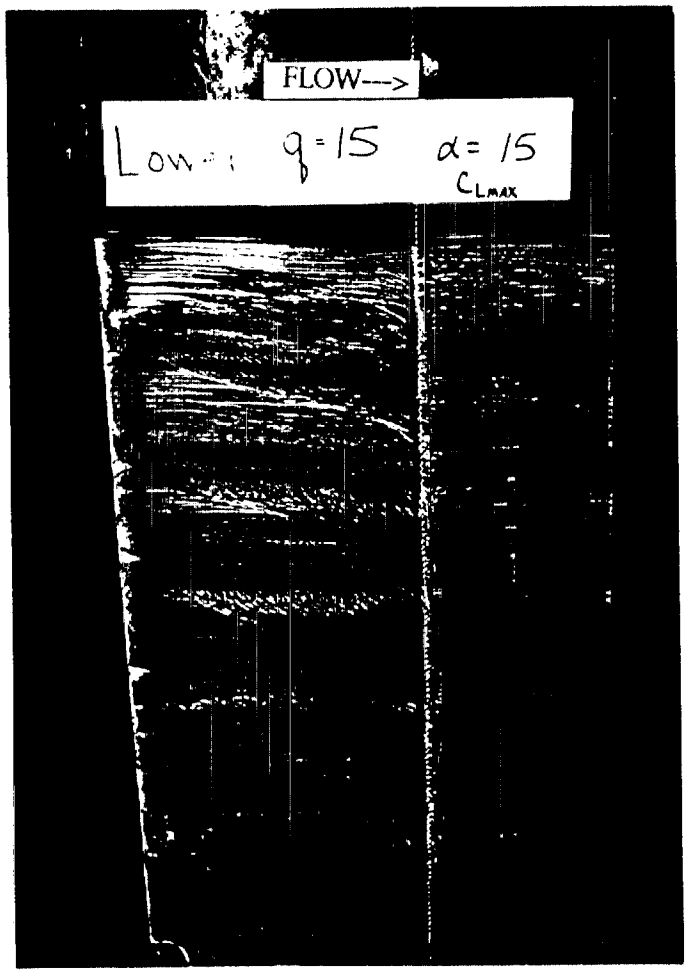

(c) α = 15°

Figure 18 - V-Tape Lower Surface Flow Visualization Photographs (RN = 1 million)

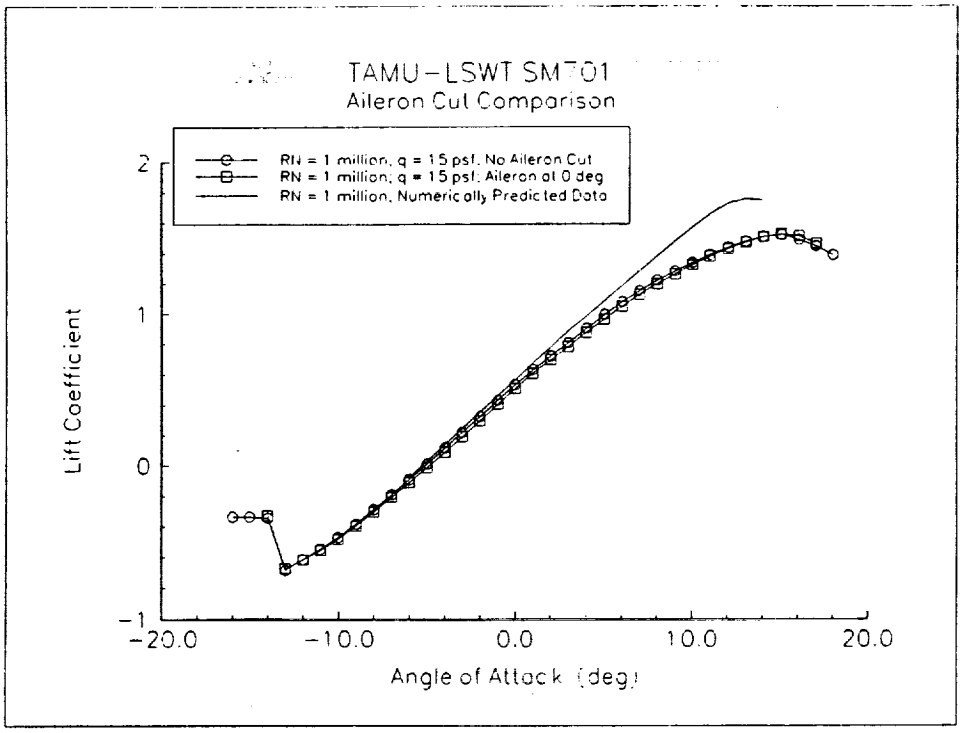

Figure 19a - Effect of Aileron Cut on Lift Coefficient (RN = 1 million)

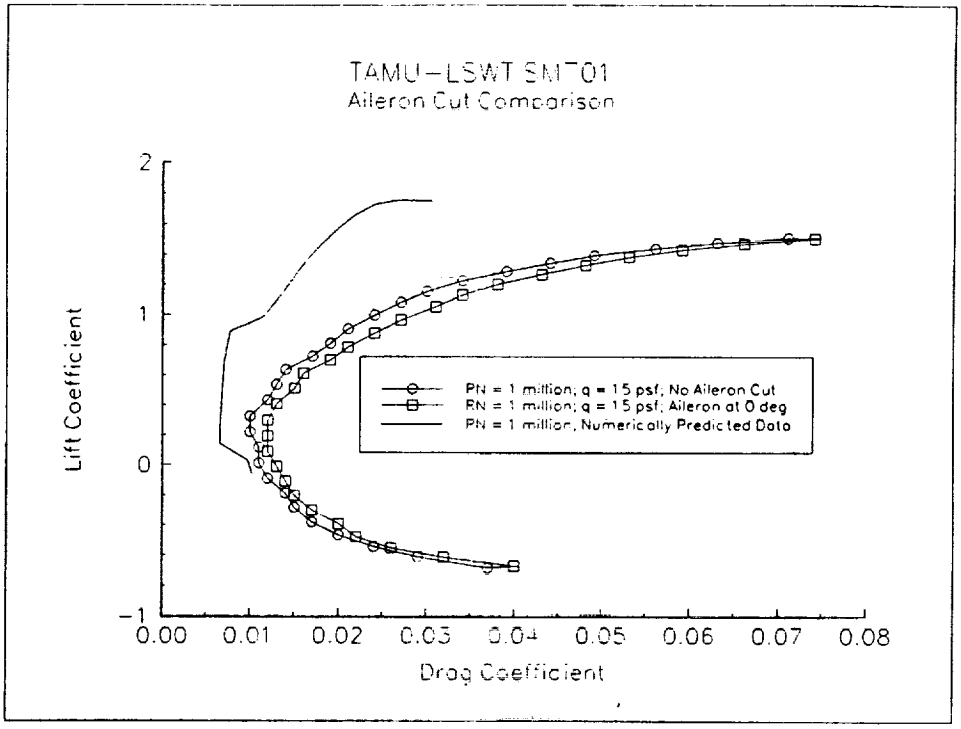

Figure 19b - Effect of Aileron Cut on Drag Coefficient (RN = 1 million)

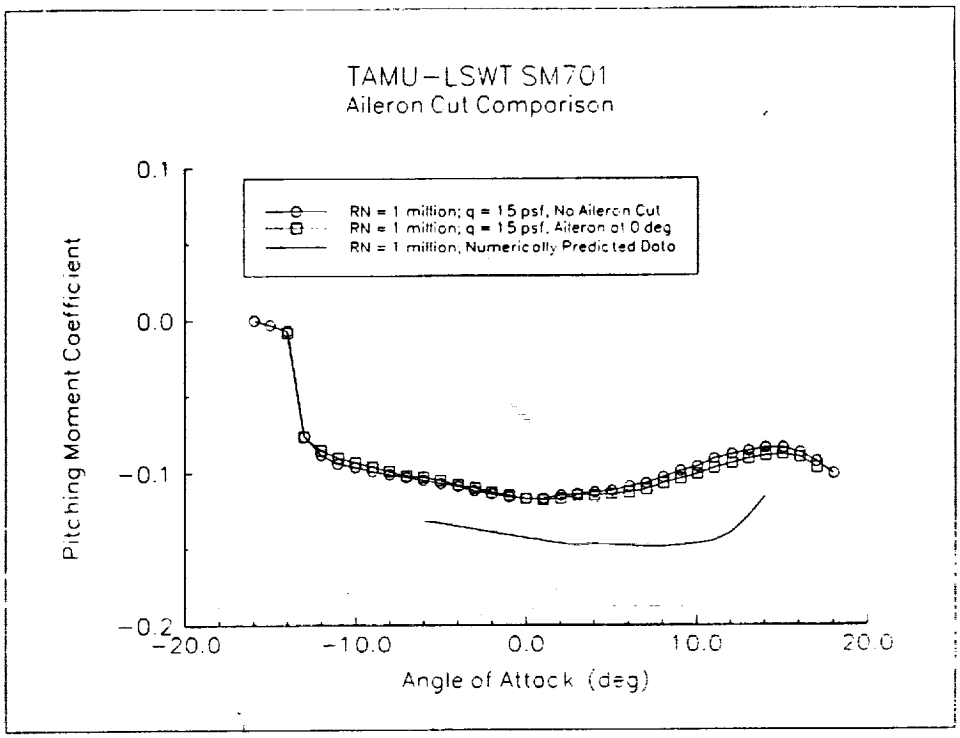

Figure 19c - Effect of Aileron Cut on Pitching Moment Coefficient (RN = 1 million)

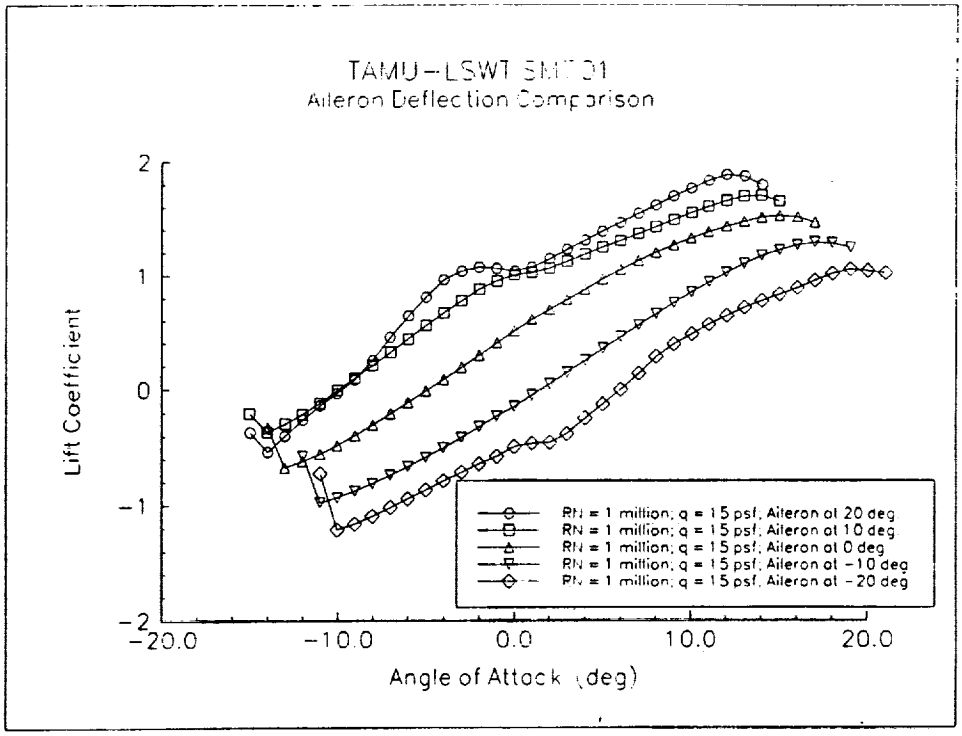

Figure 20a - Effect of Aileron Deflection on Lift Coefficient (RN = 1 million)

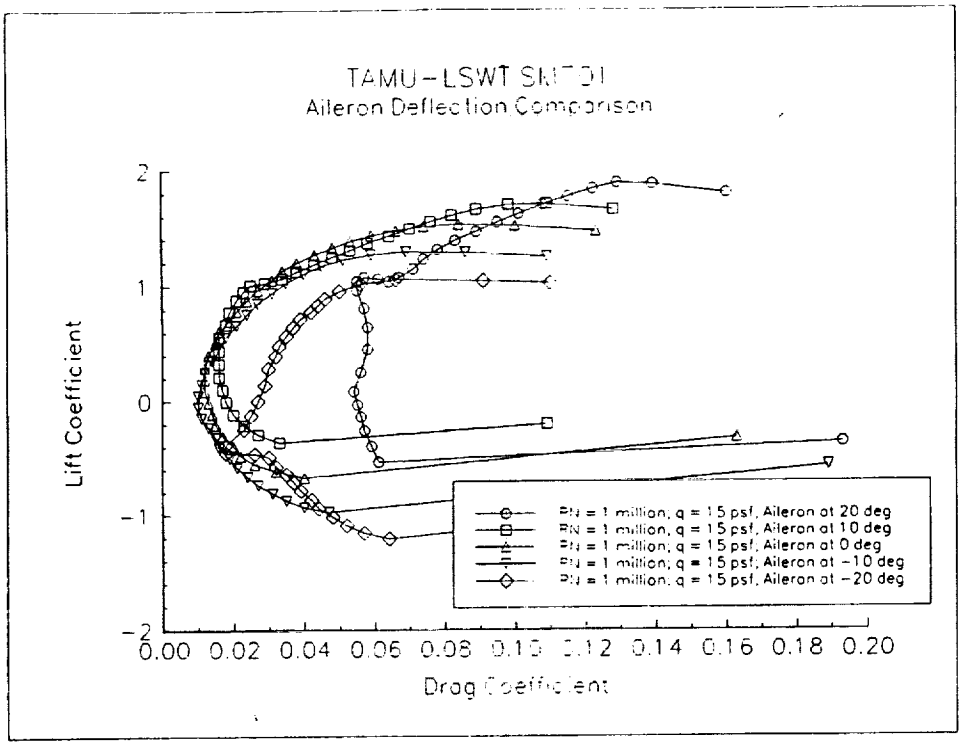

Figure 20b - Effect of Aileron Deflection on Drag Coefficient (RN = 1 million)

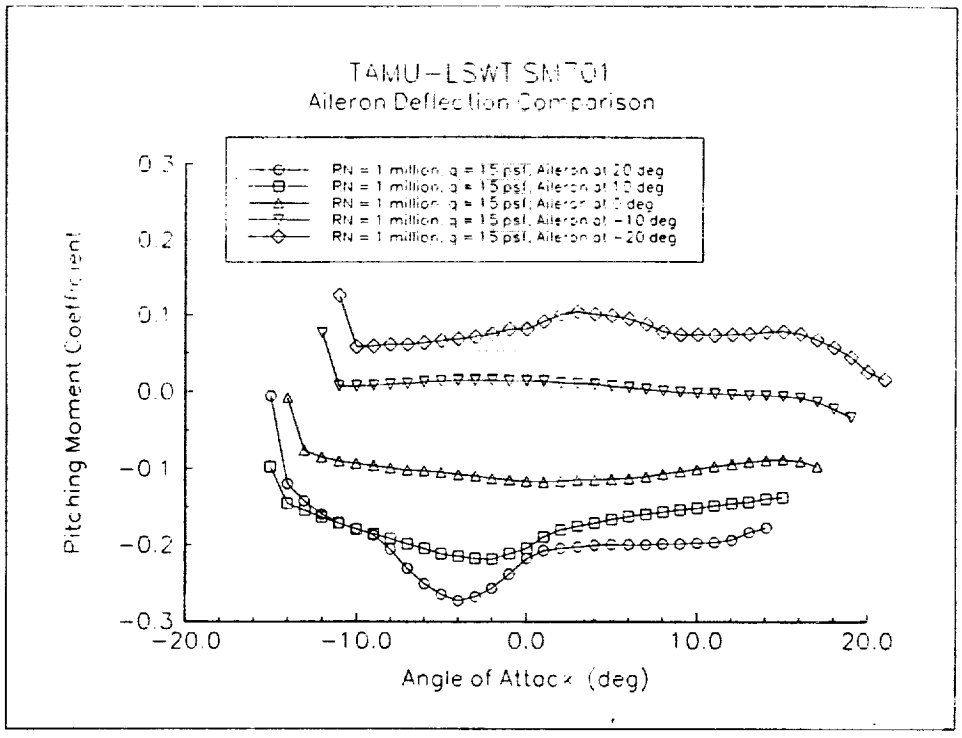

Figure 20c - Effect of Aileron Deflection on Pitching Moment Coefficient (RN = 1 million)